

Contents lists available at ScienceDirect

# Journal of the Mechanics and Physics of Solids

journal homepage: www.elsevier.com/locate/jmps



# Thermodynamics-based stability criteria for constitutive equations of isotropic hyperelastic solids



Kshitiz Upadhyay, Ghatu Subhash\*, Douglas Spearot

Department of Mechanical and Aerospace Engineering, University of Florida, Gainesville, FL 32611, United States

#### ARTICLE INFO

Article history:
Received 7 August 2018
Revised 25 September 2018
Accepted 28 September 2018
Available online 6 October 2018

Keywords: Constitutive inequalities Hyperelastic material Conservation integrals Constitutive behaviour Thermodynamic stability

#### ABSTRACT

A generalized thermodynamic stability criterion for isotropic finite elastic solids is derived using the fundamental balance laws and field equations of continuum mechanics, which is then used to formulate constitutive inequalities for the polynomial form of hyperelastic constitutive equations. Individual thermodynamic constitutive inequalities (called T-C inequalities) are derived for the neo-Hookean, Mooney Rivlin, and three-parameter generalized Rivlin models under three pure homogeneous deformation modes, namely, uniaxial compression, uniaxial tension and shear (simple and pure), and are compared against two commonly used adscititious inequalities, the Baker-Ericksen (B-E) and E-inequalities. The range of stable model constants as defined by the T-C inequalities is represented by a region in an N-dimensional coordinate space (N is the total number of model constants), which is defined as the Region of Stability (ROS). It is shown that the ROS is a function of material deformation and evolves with the limiting strain, shrinking from an initially large region representing the necessary condition of thermodynamic stability to a converged region under infinite limiting strain that is equivalent to the ROS defined by the Einequalities. By investigating the evolution of the ROS under different deformation modes, the implication of T-C inequalities on the selection of experimental routines and filtering of erroneous test data and model constants is discussed. It is also demonstrated that while the E-inequalities are over-restrictive for hyperelastic materials with small to moderate limiting strains, an observation supported by recent experimental evidence, the B-E inequalities are inaccurate under moderate to large limiting strain conditions. The applicability of the proposed mathematical framework to other hyperelastic strain energy density forms, such as exponential/logarithmic functions, is demonstrated by investigating the thermodynamic stability of the Fung-Demiray model. It is shown that the commonly assumed restriction that the Fung-Demiray model constants must be positive can be relaxed so that some typical material behaviors under small to moderate limiting strains can also be modeled.

© 2018 Elsevier Ltd. All rights reserved.

# 1. Introduction

In finite elasticity, the structure of a constitutive equation must abide by three fundamental constitutive axioms, which are (i) the principle of determinism, (ii) the principle of local action, and (iii) the principle of material frame-indifference

E-mail address: subhash@ufl.edu (G. Subhash).

<sup>\*</sup> Corresponding author.

(Noll, 1958). However, in order to ensure that the material behavior described by a constitutive equation is physically reasonable, additional restrictions have to be imposed. For example, in the linear elasticity theory for isotropic materials, the strain energy density W is not an arbitrary function, but follows certain restrictions: first, the form of W is quadratic in terms of the infinitesimal strain tensor, and second, the material parameters are restricted to ensure that W is positive definite. The latter restrictions are called the C (classical)-inequalities (Truesdell and Toupin, 1963), which restrict the limits of material parameter values and are a sufficient condition for the work theorem, stability, uniqueness and positivity of squared speeds of all possible weak waves. In terms of Poisson's ratio v and shear modulus  $\mu$ , the C-inequalities are given as

$$-1 < v < \frac{1}{2}, \quad \mu > 0$$
 (1)

In the nonlinear theory of finitely elastic materials, the problem of finding restrictions on the strain energy density function was first suggested by Truesdell (1956) as the "Hauptproblem" during a lecture in Berlin on June 1, 1955. Since then, a number of researchers have attempted to search for such restrictions based on various mechanical (empirical) and mathematical arguments, as will be elaborated upon in the following paragraphs, leading to (i) functional forms that can accurately capture the experimental data and (ii) inequalities bounding the model parameters of the functions.

The first aspect of the Hauptproblem is the selection of an ideal functional form of W, which can describe the experimental data, both qualitatively and quantitatively, with acceptable relative errors of prediction (Puglisi and Saccomandi (2016) reviewed this approach in detail). In isotropic hyperelastic materials, this involves the choice of certain invariants of the large deformation tensor (e.g.,  $I_1$ ,  $I_2$  and/or  $I_3$  invariants of the left Cauchy-Green deformation tensors **B**). Early work in this regard includes the neo-Hookean model (Rivlin, 1948a; Treloar, 1944a), which is based on the molecular (Gaussian statistical) theory and assumes purely entropic elasticity, and the Mooney-Rivlin model (Mooney, 1940; Rivlin, 1948b), which is a phenomenological model and improves fitting of experimental data over the neo-Hookean model (Saccomandi, 2018). Ogden (1972) advanced these models by using the invariants of a broader Seth-Hill family of strain measures (Hill, 1968; Seth, 1962), which allowed fitting of a wide range of deformation types. However, this introduced difficulties common with nonlinear numerical curve fitting, including multiple optimal sets of model constants that result in identical errors (Ogden et al., 2004). More recently, the formulation of semi-empirical multiscale constitutive models that relate mesoscopic deformation of polymer chains to the macroscopic material behavior has emerged, mainly by incorporating non-Gaussian effects (e.g., the Arruda-Boyce model (Arruda and Boyce, 1993) and the Gent model (Gent, 1996)). Destrade et al. (2017), based on a systematic study of the uniaxial tension behavior of rubbers, hypothesized three fundamental requirements on a reliable strain energy density function: (i) dependence on the second invariant  $I_2$ , (ii) at least three model constants, and (iii) ability to capture the limiting chain extensibility.

The search for an ideal form of the strain energy density function has highlighted the robustness of the nonlinear elasticity theory in capturing the experimental response of rubber-like materials (Treloar, 1975) under a large range of deformations, while partially bridging the gap between the mesoscopic and macroscopic deformation regimes. Such an approach, however, is based on the fitting of experimental data, whose availability is mostly limited to certain uniform deformations of rubber-like materials (e.g., uniaxial tension and equibiaxial tension). This is particularly concerning for nonlinear models, where parameters obtained from one deformation can yield poor results for other deformation types, or in a complex triaxial deformation. In addition, the experimental data itself can be marred by systematic and random error sources, in which case the reliance on such data to compare fitting of competing models can result in flawed outcomes. As will be shown later, the thermodynamics-based inequalities derived in the present work offer a method to filter out unfeasible model constants potentially resulting from numerical or experimental errors. Finally, the search for an ideal form of W, as conducted in many recent studies (Carroll, 2011; Kroon, 2011; Pucci and Saccomandi, 2002), is based on classical experimental data of conventional vulcanized rubbers (Treloar, 1944) experiments are perhaps the most common dataset in this regard). The assumption that the mechanical behavior of these "conventional" hyperelastic materials in every deformation mode is qualitatively similar to that exhibited by novel materials described by hyperelastic constitutive equations (e.g., biological tissues (Casaroli et al., 2017; Mihai et al., 2017) and gelatin (Czerner et al., 2015; Tang et al., 1997)) needs further investigation.

The second aspect of the Hauptproblem deals with the formulation of mathematical restrictions on the model constants (or response coefficients) of the strain-energy density function W (or the free energy  $\psi$  (Haupt, 2002)) or its generalized form, so that the predicted material behavior is physically reasonable. For example, consider the Rivlin-Ericksen representation of Cauchy stress tensor  $\sigma$  (obtained by differentiating W with respect to the strain tensor), given by

$$\sigma = s_0 \mathbf{1} + s_1 \mathbf{B} + s_2 \mathbf{B}^{-1} \tag{2}$$

where **1** is the unit symmetric tensor, and  $s_0$ ,  $s_1$  and  $s_2$  are the response coefficients. The response coefficients in Eq. (2) are related to W by

$$s_0 = \frac{2}{\sqrt{I_3}} \left( I_2 \frac{\partial W}{\partial I_2} + I_3 \frac{\partial W}{\partial I_3} \right), \ s_1 = \frac{2}{\sqrt{I_3}} \left( \frac{\partial W}{\partial I_1} \right), \ s_2 = -2\sqrt{I_3} \left( \frac{\partial W}{\partial I_2} \right)$$
 (3)

Unlike the linear elasticity theory of isotropic materials where model constants are bounded by the well-defined C-inequalities, the formulation of restrictive inequalities for isotropic nonlinear finitely elastic materials is a non-trivial task because the response coefficients are scalar functions of material deformation. Early proposals in this regard include Truesdell (1952) condition, which is necessary and sufficient for positive work when one principal extension is increased

while another is kept fixed,

$$\frac{\partial W}{\partial I_1} + \lambda_i^2 \frac{\partial W}{\partial I_2} \ge 0, \quad i = 1, \quad 2, \quad 3$$
 (4)

where  $\lambda_i$  are the principal stretches (i.e., eigenvalues of the right and left stretch tensors). Baker and Ericksen (1954) proposed that Eq. (4) is equivalent to the empirical requirement that the greater principal stress occurs in the direction of the greater principal stretch, except that the non-strict inequality was replaced by a strict inequality. The mathematical form of the resulting B-E inequality is

B-E: 
$$s_1 - \frac{1}{\lambda_a^2 \lambda_b^2} s_2 > 0$$
,  $\lambda_a \neq \lambda_b$ ,  $a, b = 1, 2, 3$  (5)

Another common inequality called the Ordered-Force (O-F) inequality resulted as a consequence of the Coleman-Noll (C-N) condition (Coleman and Noll, 1959) of restricted convexity of the strain-energy function, and requires that the greater stretch will always occur in the direction of the greater force.

$$O-F: -\frac{1}{\lambda_a \lambda_b} s_0 + s_1 - \frac{\lambda_a^2 + \lambda_a \lambda_b + \lambda_b^2}{\lambda_a^3 \lambda_b^3} s_2 > 0, \ \lambda_a \neq \lambda_b, \ a, b = 1, \ 2, \ 3$$
 (6)

The B-E and O-F inequalities are part of a group of restrictive inequalities known as adscititious inequalities, for they cannot be directly derived from first principles and are based on common experience and experimental evidence. A stronger form of inequality that implies both the B-E and O-F inequalities was proposed by Truesdell and Toupin (1963), and is known as the empirical (E) inequality. The mathematically equivalent form of the E-inequality is

$$E: s_0 < 0, \ s_1 > 0, \ s_2 < 0$$
 (7)

Adscititious inequalities have been strongly supported by a number of experiments on rubber-like materials (called Green-elastic or hyperelastic materials) and are oftentimes regarded as fundamental laws (Mihai and Goriely, 2011). This is partly because the mathematical inequalities are based on some common physical notion (adscititious inequalities) or on thermodynamics-based principals, as opposed to the mechanical approach that relies on fitting specific forms of W on experimental data of certain rubbers in special deformation modes. This quality of being independent of experimental data, material type, numerical fitting procedure, or any particular form of W makes them an invaluable tool that impose additional restrictions on a recommended constitutive model.

The validity of some of these inequalities, however, has been questioned. For example, Rivlin (1973) and Lee (1973) pointed out that the Coleman-Noll (C-N) inequality results in a unique stable equilibrium configuration when applied to the pure homogeneous deformation of an isotropic elastic material of cubic dimensions, which directly conflicts with the earlier findings of Rivlin (1948c) that showed multiple possible equilibrium configurations for certain ranges of applied forces. McLellan (1975) demonstrated that the effect of isotropy group of a material was not fully considered in Coleman and Noll's postulate, and thus the proof of the O-F inequalities is invalid and the postulate itself needs to be modified. Moreover, Marzano (1983) proved that for a finite elastic material in uniaxial tension that follows B-E inequalities, if the first E-inequality ( $s_0 \le 0$ ) holds, then the second one ( $s_1 > 0$ ) necessarily holds as well. However, nothing can be said about the third E-inequality ( $s_2 \le 0$ ). Moon and Truesdell (1974) demonstrated that for a material under shear that follows E-inequalities, negative Poynting effect (i.e., when sheared faces tend to come close together) is not physically possible. However, recent experimental evidence (Janmey et al., 2007) has suggested that semiflexible polymeric gels exhibit negative Poynting effect under simple shear deformation. Theoretical analysis in several studies (e.g., Destrade et al., 2015; Horgan and Murphy, 2015; Mihai and Goriely, 2011) revealed that E-inequalities are excessively restrictive for shear deformation in biopolymers. Compression studies on soft polymers have also shown that E-inequalities do not necessarily hold true in these systems (Leclerc et al., 2012; Sasson et al., 2012). Formulation of a theoretically motivated set of inequalities that neither over-constrain a constitutive model, nor are too weak to allow impractical material responses, is thus much needed. As commented by Ball and James (2002), there are perhaps no generalized fundamental mathematical restrictions on the form of the strain-energy function that guarantee a reasonable mechanical behavior in every possible situation. Nevertheless, the very search for such restrictions has, over the years, stimulated interest in researchers from a wide range of backgrounds (e.g., material scientists, mathematicians, engineers, etc.), resulting in deep insights, although partial, on the strain-energy density functional forms, model behaviors, and the finite theory of elasticity in general.

Thus, the objective of the present work is to formulate thermodynamics-based restrictions on the model constants of strain energy density functions for isotropic hyperelastic solids. To this end, this work leverages recent contributions by Liu (2012), who derived an inequality for the two-parameter Mooney-Rivlin solid under isothermal uniaxial deformation, to derive a tensorial form of thermodynamic stability criterion in Section 2.

Liu (2012) demonstrated using the second law of thermodynamics that E-inequalities can be relaxed and only a single inequality is necessary to ensure thermodynamic stability,

$$s_1 > s_2 \tag{8}$$

Although insightful, this result is rather limited in application in that only a particular deformation mode and a particular hyperelastic model were considered, whereas a set of six pure homogeneous deformation modes (also called primary

deformation modes) are generally required for the estimation of model constants (Ogden, 1972; Ogden et al., 2004). In the case of incompressible materials, pairs of these deformation modes, namely, uniaxial tension and equibiaxial compression, uniaxial compression and equibiaxial tension, and pure shear and planar compression, follow theoretical equivalence relations, so that only three primary deformation modes (one from each pair) have to be considered (Berselli et al., 2011). Therefore, in Section 3, the requirement of thermodynamic stability is extended to cover the broader class of polynomial hyperelastic models under the three primary deformation modes (uniaxial tension, uniaxial compression and pure shear). These models are based on the Rivlin-Signorini method that approximates the strain energy density in terms of a power series of the polynomial functions of appropriate invariants (Rivlin, 1997; Signorini, 1955),

$$W(I_1, I_2) = \sum_{m+n=1}^{\infty} A_{mn} (I_1 - 3)^m (I_2 - 3)^n$$
(9)

where  $A_{mn}$  are the hyperelastic model constants. In an important contribution of this research, it will be demonstrated that the constitutive inequalities depend on not only the response functions or hyperelastic model constants, but also on the model type, deformation mode and limiting material strain. The latter parameter is defined as the maximum strain after which the specimen starts to exhibit softening behavior or fails, and a unique stress-strain relation no longer exists. An understanding of the effect of this parameter on the thermodynamic stability of a hyperelastic constitutive model is important, especially because an entire class of semi-empirical models (Beatty, 2008) for materials exhibiting limiting molecular chain extensibility (e.g., Gent-Gent model (Pucci and Saccomandi, 2002) and Puso model (Beatty, 2003)) contain some variant of limiting strain parameter imbedded in their form.

Although simple models such as the first two approximations of the Rivlin-Signorini method provide direct relations between model constants and response coefficients, response functions of higher order polynomial models and exponential/logarithmic models (e.g., Fung-Demiray (Demiray, 1972; Fung, 1967) and Arruda-Boyce (Arruda and Boyce, 1993)) are more complicated functions of hyperelastic model constants. Inequalities such as Eq. (8) are thus not suitable in these cases for defining bounds on the model constants, which are undeniably more commonly used in modern FEA packages and simulation software (*Abaqus v6.12 Analysis User's Manual*, 2012) than response coefficients. In Section 4, thermodynamic constitutive inequalities in terms of model constants are derived for three common polynomial hyperelastic models, namely, neo-Hookean, Mooney-Rivlin, and three-parameter generalized Rivlin models, and the implication of these restrictions on the design of experimental routines for obtaining model constants is discussed. This is especially important in hydrogels and biological tissue research where conducting certain mechanical tests (e.g., tension and shear) is difficult and sometimes infeasible due to the slippery and fragile nature of specimens. In addition, the variation of the stability restrictions with limiting strain under different deformation modes is investigated. The bounds on model constants so obtained using the thermodynamics-based approach are compared with those derived using adscititious B-E and E-inequalities, which provides clues about their experimental success and a possible thermodynamic justification.

The mathematical framework setup in this work is not at all limited to the polynomial class of models and can be applied to other strain-energy density forms (e.g., non-polynomial models yielded by the modified Rivlin-Signorini scheme (Horgan and Saccomandi, 2003)). As an example, in Section 5, bounds on model constants of the exponential Fung-Demiray model are derived using the thermodynamics-based approach outlined in this work.

#### 2. Thermodynamic stability criterion

As shown in Eq. (2), the stress in an isotropic Cauchy-elastic solid can be expressed in the form of the left Cauchy-Green deformation tensor **B** with respect to some natural or equilibrium configuration. Cauchy-elastic solids in which a path-independent strain-energy density function exists are called Green-elastic or hyperelastic materials. In other words, the strain energy density W in an isotropic hyperelastic solid is a function of only the instantaneous finite strain tensor **E** (**C** or **B** may also be used as in Eq. (9), where principal invariants of these tensors are the independent variables). In this section, building upon and generalizing the work of Liu (2012), a thermodynamic stability criterion is derived for an isotropic hyperelastic solid using the fundamental balance equations of continuum mechanics. Other elastic materials (including elastic fluids, which do not have a natural ground state) as well as dispersive phenomena such as dynamic viscoelastic deformations are thus not in the scope of present work.

Starting with the conservation of energy and the Clausius-Duhem entropy inequality in continuum mechanics,

$$\frac{d}{dt} \int_{\Omega(t)} \rho\left(\frac{1}{2}\mathbf{v} \cdot \mathbf{v} + u\right) dV - \int_{\Omega(t)} \rho(r + \mathbf{b} \cdot \mathbf{v}) dV + \int_{\partial \Omega(t)} (\mathbf{q} \cdot \mathbf{n} - \mathbf{t} \cdot \mathbf{v}) d\mathbf{a} = 0$$
(10a)

$$\frac{d}{dt} \int_{\Omega(t)} \rho \eta dV + \int_{\partial \Omega(t)} \frac{\mathbf{q}}{\theta} \cdot \mathbf{n} d\mathbf{a} - \int_{\Omega(t)} \rho \frac{r}{\theta} dV \ge 0 \tag{10b}$$

where  ${\bf v}$  is the velocity vector, u is the specific internal energy,  $\rho$  is the mass density,  ${\bf r}$  is the rate of internal heating per unit mass,  ${\bf b}$  is the body force,  ${\bf q}$  is the heat flux,  ${\bf n}$  is the outward normal to the surface  $\partial \Omega({\bf t})$  that bounds volume  $\Omega({\bf t})$ ,  ${\bf t}$  is the traction vector,  $\eta$  is the specific entropy, and  $\theta$  is the absolute temperature. Elimination of  ${\bf q}$  and  ${\bf r}$  by subtracting

Eq. (10b) from Eq. (10a) and the introduction of the Helmholtz free energy function  $\psi = u - \theta \eta$  yields

$$\frac{d}{dt} \int_{\Omega(t)} \rho\left(\frac{1}{2}\mathbf{v} \cdot \mathbf{v} + \psi\right) dV - \int_{\Omega(t)} \rho\left(\mathbf{b} \cdot \mathbf{v}\right) dV - \int_{\partial\Omega(t)} \mathbf{t} \cdot \mathbf{v} d\mathbf{a} \le 0$$
(11)

Using the Reynold's transport theorem on the first term and the divergence theorem on the second term of Eq. (11),

$$\int_{\Omega(t)} \left( \rho \frac{d\psi}{dt} + \rho \left( \mathbf{v} \cdot \frac{d\mathbf{v}}{dt} \right) - \rho \left( \mathbf{b} \cdot \mathbf{v} \right) - \nabla \cdot (\boldsymbol{\sigma} \cdot \mathbf{v}) \right) dV \le 0$$
(12)

Expanding the last term in the integrand of Eq. (12) and invoking the conservation of linear momentum,

$$\int_{\Omega(t)} \left( \rho \frac{d\psi}{dt} + \rho \left( \mathbf{v} \cdot \frac{d\mathbf{v}}{dt} \right) - \rho \left( \frac{d\mathbf{v}}{dt} \cdot \mathbf{v} \right) - \boldsymbol{\sigma} \cdot \cdot \mathbf{L} \right) dV \le 0$$
(13)

where **L** is the velocity gradient tensor, and the symbol  $\cdots$  defines an alternative definition of tensor scalar product (Malvern, 1969), such that  $\sigma \cdot \mathbf{L} = \sigma_{ij} L_{ji}$  in rectangular Cartesians. In the absence of couple stresses, the Cauchy stress tensor is symmetric (conservation of angular momentum). Thus, Eq. (13) becomes

$$\int_{\Omega(t)} \left( \rho \frac{d\psi}{dt} - \boldsymbol{\sigma} : \mathbf{D} \right) dV \le 0 \tag{14}$$

where **D** is the rate of deformation tensor with respect to the reference state, and the tensor scalar product is  $\sigma : \mathbf{D} = \sigma_{ij}D_{ij}$  in rectangular Cartesians. Transforming the integral in Eq. (14) to the reference configuration gives

$$\int_{\Omega_0} \left( \frac{d(\rho_0 \psi)}{dt} - \mathbf{T}_0^{\mathsf{T}} : \dot{\mathbf{F}} \right) dV_0 \le 0 \tag{15}$$

where  $\mathbf{T}_0$  is the first Piola-Kirchhoff stress tensor,  $\dot{\mathbf{F}}$  is the time rate of change of the deformation gradient tensor, and  $\rho_0$  is the mass density of the initial undeformed volume  $V_0$  (reference configuration). The local forms of Eqs. (14) and (15) are

$$\frac{d\psi}{dt} - \frac{\mathbf{\sigma}}{\rho} : \mathbf{D} \le 0; \quad \frac{d\psi}{dt} - \frac{\mathbf{T}_0^{\mathrm{T}}}{\rho_0} : \dot{\mathbf{F}} \le 0$$
 (16)

In Eq. (16), the first term is the rate of change of the Helmholtz free energy, and the second term is the specific thermodynamic stress power. Liu (2012), in his derivation of the thermodynamic stability criterion for a Mooney-Rivlin material under uniaxial deformation, defined their difference as the rate of change of *available energy*  $\phi$  in the system. Thus, for any isotropic hyperelastic material,

$$\frac{d}{dt}\rho(\psi - \Pi) = \frac{d\phi}{dt} \le 0 \tag{17}$$

where  $\Pi$  is the specific energy input from external forces, which does not contribute to the kinetic energy of the system, and is related to the available energy as  $\phi = \rho(\psi - \Pi)$ . Mathematically,

$$\Pi = \int_0^t \frac{\mathbf{T}_0^{\mathsf{T}}}{\rho_0} : \dot{\mathbf{F}} dt = \int_0^t \frac{\boldsymbol{\sigma}}{\rho} : \mathbf{D} dt \tag{18}$$

Eq. (17) is a monotonically decreasing function in time. Thus, for an arbitrary stable state at time t and deformation gradient  $\mathbf{F}$ , any small perturbation  $\delta \mathbf{u}$  will eventually return to this state, that is,

$$(\nabla \phi) \cdot \delta \hat{\mathbf{u}} = 0 \tag{19}$$

In Eq. (19), the left side of the equation is the directional derivative of the available energy function in the direction of  $\delta \mathbf{u}$  ( $\delta \hat{\mathbf{u}}$  being the unit vector in the direction of  $\delta \mathbf{u}$ ). Eq. (19) will give the critical point at which the available energy attains its extremum value. However, to ensure that this is a local minimum, a second order derivative test can be performed (e.g., Hessian matrix test).

Thus, a given set of hyperelastic model constants are thermodynamically stable at a particular state of deformation if the available energy attains its minimum at this state. Eq. (16) to Eq. (19) will now be used to derive thermodynamic stability criteria for hyperelastic models of polynomial form under a variety of primary deformation modes. Note that these stability criteria are applicable to a particular hyperelastic model only if the mechanical characterization experiments conducted to obtain its model constants are quasi-static, i.e., the equilibrium equations are satisfied and thus the stress-strain data represents actual material response and not the inertia effects.

# 3. Bounds on polynomial hyperelastic model constants and the region of stability

In this section, the thermodynamic stability criterion is used to define limits on the model constants in polynomial hyperelastic models. A general polynomial form of the hyperelastic strain energy density function is given by the following Taylor series expansion (Kim, 2015)

$$W(I_1, I_2) = \sum_{m+n=1}^{\infty} A_{mn} (I_1 - 3)^m (I_2 - 3)^n = A_{10} (I_1 - 3) + A_{01} (I_2 - 3) + A_{11} (I_1 - 3) (I_2 - 3) + \mathcal{O}((I_1 - 3)^2, (I_2 - 3)^2)$$

$$(20)$$

where  $\mathcal{O}$  is the Bachmann-Landau (big 0) notation, which represents the higher order error terms in a Taylor expansion, and  $A_{mn}$  are model constants, which are derived numerically from experimental data (Beda, 2014; Mansouri and Darijani, 2014). Eq. (20) is a powerful form as it is not only independent of the type of invariants used, but also provides a general framework for obtaining particular strain-energy density forms in terms of constant coefficients rather than variable response coefficients (Horgan and Saccomandi, 2003). In addition, this form assumes material incompressibility (W is independent of  $I_3$ ), which is a common assumption for most hydrogels and biological tissues under their typical limiting strains as they are composed of mostly water (Normand et al., 2000; Pavan et al., 2010; Tang et al., 1997; Trinh et al., 2009; Wex et al., 2015).

A form similar to Eq. (20) can be used to describe the Helmholtz free energy function  $\psi$  as given by

$$\psi(\theta, l_1, l_2) = \psi_{00} + \psi_{10}(l_1 - 3) + \psi_{01}(l_2 - 3) + \psi_{11}(l_1 - 3)(l_2 - 3) + \mathcal{O}((l_1 - 3)^2, (l_2 - 3)^2)$$
(21)

Under isothermal deformation and reversible heat transfer conditions, functions W and  $\psi$  are related as (Malvern, 1969)

$$\mathbf{S} = \frac{\partial W}{\partial \mathbf{E}} = \rho_0 \left( \frac{\partial \psi}{\partial \mathbf{E}} \right)_{\theta} \tag{22}$$

where S is the second Piola-Kirchhoff stress tensor. From Eqs. (20) – (22), the hyperelastic model constants can be related to the coefficients of invariants in the free energy function (Eq. (21)) as

$$A_{mn} = \rho_0 \psi_{mn} \tag{23}$$

For a general polynomial hyperelastic model Eq. (20) or (21), the second order derivative test for minimization criterion results in a general form of the thermodynamic constitutive inequality (T-C inequality) given by

$$\sum_{m+n=1}^{\infty} A_{mn} \zeta_{mn}(\varepsilon) > 0 \tag{24}$$

where  $A_{mn}$  are hyperelastic model parameters, and  $\zeta_{mn}(\varepsilon)$  are corresponding functions of some strain measure (e.g., stretch for uniaxial case and shear strain for simple/pure shear). When plotted in an N-dimensional coordinate space (N being the total number of model constants) with  $A_{mn}$  in the respective axes, Eq. (24) represents an open half-space where hyperelastic model constants are thermodynamically stable. In this work, the intersection of half spaces obtained at different limiting strains (undeformed to strain at maximum stress) and deformation modes is defined as the *Region of Stability (ROS)*. Note that T-C inequalities are the constitutive inequalities that define the *ROS*, that is, the coordinate open half-space where model constants are stable (or feasible).

In the following subsections, the T-C inequalities for a general polynomial hyperelastic model (Eq. (20)) under primary deformation modes of compression, tension and shear are derived.

# 3.1. Uniaxial deformation (compression and tension)

Referring to Fig. 1, the boundary conditions for uniaxial compression and tension are zero traction on lateral free surfaces, and zero and a constant velocity of boundaries  $x_1 = 0$  and  $x_1 = L$ , respectively.

$$\mathbf{v}|_{\mathbf{x},=0} = \mathbf{0}, \quad \mathbf{v}|_{\mathbf{x},=l} = \dot{\lambda} L_0 \mathbf{e}_1 \tag{25}$$

where  $\lambda$  is the principal stretch ( $\lambda = L/L_0$ ) in the  $\mathbf{e}_1$  direction (standard basis { $\mathbf{e}_1$ ,  $\mathbf{e}_2$ ,  $\mathbf{e}_3$ }). The only non-zero term in the  $\mathbf{T}_0$  tensor is the 1-1 component,  $T_{11} = F/A_0$ ; thus, Eqs. (16) and (17) can be combined to obtain the rate of change of *available energy*  $\phi$  for a homogeneous material under quasi-static uniaxial deformation as

$$\frac{d}{dt}(\rho_0\psi - T_{11}\lambda) = \frac{d\phi_U(\lambda)}{dt} \le 0 \tag{26}$$

where subscript U on  $\phi$  denotes uniaxial deformation mode. Note that the left-hand side of Eq. (26) is the rate of change of the difference between the free energy and the potential energy, which is also the rate of change of available energy (refer to Eq. (17)).

From Eq. (26), it is obvious that an arbitrary state of deformation  $\lambda$  is stable when the available energy function  $\phi$  attains its minimum value at this state. Thus, the thermodynamic stability criterion becomes

$$\frac{d\phi_U(\lambda)}{d\lambda} = 0, \qquad \frac{d^2\phi_U(\lambda)}{d\lambda^2} > 0 \tag{27}$$

In uniaxial deformation, the tensor C and its principal invariants take the form given by

$$\mathbf{C} = \begin{bmatrix} \lambda^2 & 0 & 0 \\ 0 & \frac{1}{\lambda} & 0 \\ 0 & 0 & \frac{1}{\lambda} \end{bmatrix}, \quad I_1 = \lambda^2 + \frac{2}{\lambda}, \quad I_2 = 2\lambda + \frac{1}{\lambda^2}$$
 (28)

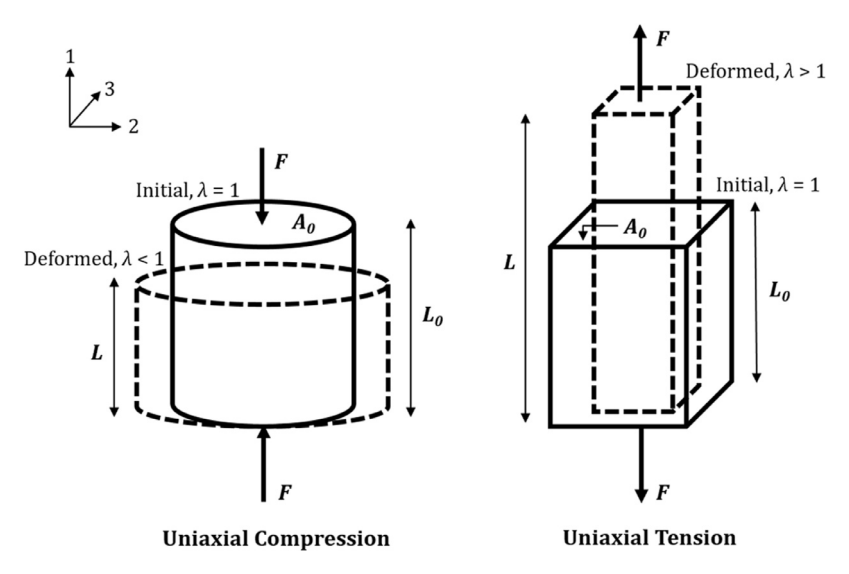


Fig. 1. A schematic illustration of uniaxial deformation modes: compression and tension.

Substituting the general polynomial Helmholtz free energy from Eqs. (21) and (28) into the thermodynamic stability criterion (Eq. (27)),

$$\frac{d\phi_{U}(\lambda)}{d\lambda} = 2\rho_{0}\psi_{10}\left(\lambda - \frac{1}{\lambda^{2}}\right) + 2\rho_{0}\psi_{01}\left(\frac{1}{\lambda^{3}} - 1\right) + 6\rho_{0}\psi_{11}\left(\lambda^{2} - \lambda - \frac{1}{\lambda^{4}} + \frac{1}{\lambda^{3}} + \frac{1}{\lambda^{2}} - 1\right) + \mathcal{O}\left((I_{1} - 3)^{2}, \quad (I_{2} - 3)^{2}\right) - T_{11} = 0$$
(29)

Rearranging Eq. (29) and using Eq. (23) to replace free energy coefficients yields the familiar equation for uniaxial nominal stress in a polynomial hyperelastic model as given by

$$T_{11} = 2A_{10}\left(\lambda - \frac{1}{\lambda^2}\right) + 2A_{01}\left(1 - \frac{1}{\lambda^3}\right) + 6A_{11}\left(\lambda^2 - \lambda - \frac{1}{\lambda^4} + \frac{1}{\lambda^3} + \frac{1}{\lambda^2} - 1\right) + \mathcal{O}\left((I_1 - 3)^2, (I_2 - 3)^2\right) \tag{30}$$

Using the second stability condition of Eq. (27),

$$\frac{d^2\phi_U(\lambda)}{d\lambda^2} = 2A_{10}\left(1 + \frac{2}{\lambda^3}\right) + 2A_{01}\left(\frac{3}{\lambda^4}\right) + 6A_{11}\left(2\lambda - 1 + \frac{4}{\lambda^5} - \frac{3}{\lambda^4} - \frac{2}{\lambda^3}\right) + \mathcal{O}\left((I_1 - 3)^2, (I_2 - 3)^2\right) > 0 \tag{31}$$

which is the T-C inequality that defines the ROS of polynomial hyperelastic models under uniaxial deformation.

#### 3.2. Simple shear

In the simple shear case as illustrated in Fig. 2, the boundary conditions are zero traction on top and bottom free surfaces, and zero and a constant velocity at boundaries  $x_2 = 0$  and  $x_2 = B_0$ , respectively.

$$\mathbf{v}|_{X_{2}=0} = \mathbf{0}, \ \mathbf{v}|_{X_{2}=B_{c}} = \dot{\gamma} B_{o} \mathbf{e}_{1}$$
 (32)

where  $\gamma$  is the nominal shear strain ( $\gamma = \Delta/B_0$ ). This time, the only non-zero component in the deformation gradient tensor **F** is the 1-2 component,  $F_{12} = \dot{\gamma}$ . Eqs. (16) and (17) can thus be combined to obtain the rate of change of *available energy*  $\phi$  under quasi-static simple shear deformation as

$$\frac{d}{dt}(\rho_0\psi - T_{21}\gamma) = \frac{d\phi_{SS}(\gamma)}{dt} \le 0 \tag{33}$$

where  $T_{21} = F/A_0$  and  $\phi_{SS} = (\rho_0 \psi - T_{21} \gamma)$  are the 2-1 component of the  $\mathbf{T}_0$  tensor and the available energy in simple shear, respectively. Note that unlike the uniaxial deformation case where  $T_{11}$  was the only non-zero stress component, simple shear deformation results in a complex multiaxial stress state (Destrade et al., 2012). However, only the shear component  $T_{21}$  contributes to the stress power ( $T_{21}$  component is parallel to the shear deformation). A similar conclusion can be reached by calculating the contraction of Cauchy stress tensor  $\sigma$  and the rate of deformation tensor  $\mathbf{D}$  (Eq. (14)). In that case, the 1-2 component of  $\mathbf{D}$  comes out to be the only non-zero component ( $T_{21} = \gamma$ ).

Finally, the thermodynamic stability criterion for simple shear can be written as

$$\frac{d\phi_{SS}(\gamma)}{d\gamma} = 0, \quad \frac{d^2\phi_{SS}(\gamma)}{d\gamma^2} > 0 \tag{34}$$

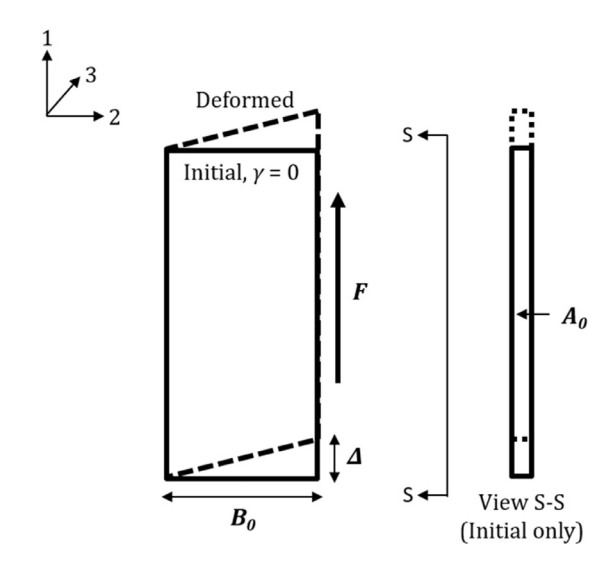


Fig. 2. Illustration of the simple shear deformation state.

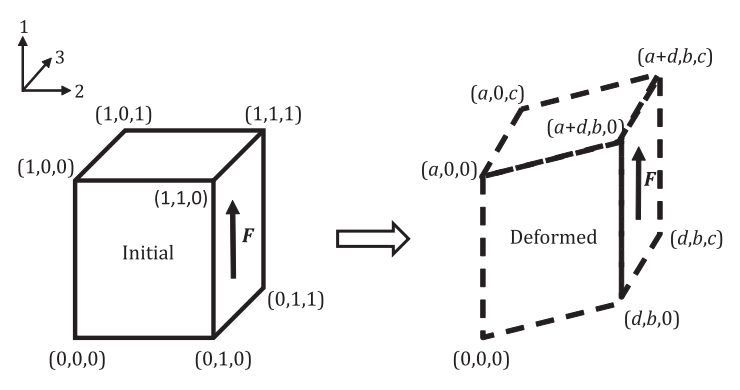


Fig. 3. Illustration of the reference and deformed states under pure shear deformation.

In simple shear, the tensor C and its principal invariants are

$$\mathbf{C} = \begin{bmatrix} 1 & \gamma & 0 \\ \gamma & \gamma^2 + 1 & 0 \\ 0 & 0 & 1 \end{bmatrix}, \quad I_1 = \gamma^2 + 3, \quad I_2 = \gamma^2 + 3$$
 (35)

By substituting principal invariants from Eq. (35) in the Helmholtz free energy function (Eq. (21)) and employing the first stability criterion of Eq. (34), the 1–2 component of the  $T_0$  tensor is

$$T_{21} = 2\rho_0 \psi_{10} \gamma + 2\rho_0 \psi_{01} \gamma + 4\rho_0 \psi_{11} \gamma^3 + \mathcal{O}((I_1 - 3)^2, (I_2 - 3)^2)$$
(36)

Using the second stability condition of Eq. (34) and the material parameters in Eq. (23),

$$\frac{d^2\phi_{SS}(\gamma)}{d\gamma^2} = 2A_{10} + 2A_{01} + 12A_{11}\gamma^2 + \mathcal{O}((I_1 - 3)^2, (I_2 - 3)^2) > 0$$
(37)

which is the T-C inequality for the ROS of a polynomial hyperelastic model under simple shear.

#### 3.3. Pure shear

Fig. 3 shows the reference and deformed configuration of an initial cube under pure shear. This general pure shear deformation is more complex as compared to the simple shear case because the traction boundary condition is now given by a time-dependent non-zero traction vector in the  $\mathbf{e}_1$  direction, and the velocity is a multidirectional vector on both the left and right shearing faces. Mathematically, the velocity boundary conditions are given by

$$\mathbf{v}|_{X_2=0} = \dot{a}X_1\mathbf{e}_1 + \dot{c}X_3\mathbf{e}_3, \qquad \mathbf{v}|_{X_2=1} = \left(\dot{a}X_1 + \dot{d}\right)\mathbf{e}_1 + \dot{b}\mathbf{e}_2 + \dot{c}X_3\mathbf{e}_3 \tag{38}$$

The Cauchy stress state in the pure shear condition is

$$\sigma = \begin{bmatrix} 0 & \frac{F}{A} & 0 \\ \frac{F}{A} & 0 & 0 \\ 0 & 0 & 0 \end{bmatrix}, \quad A = ac$$
 (39)

Because of the simplicity of the Cauchy stress tensor in this case, it is convenient to use the deformed configuration form of *available energy* (first part of Eq. (16)) to derive the thermodynamic stability criterion. Starting with the relation between reference and deformed configuration,

$$x_1 = aX_1 + dX_2$$

$$x_2 = bX_2$$

$$x_3 = cX_3$$
(40)

where  $d^2 = a^2 - b^2$ . Using Eq. (40), the tensors **F** and **L** are obtained as

$$\mathbf{F} = \begin{bmatrix} a & \sqrt{a^2 - b^2} & 0 \\ 0 & b & 0 \\ 0 & 0 & c \end{bmatrix} \tag{41}$$

$$\mathbf{L} = \dot{\mathbf{F}} \cdot \mathbf{F}^{-1} = \begin{bmatrix} \frac{\dot{a}}{a} & \left( \frac{a\dot{a} - b\dot{b}}{b\sqrt{a^2 - b^2}} - \frac{\dot{a}\sqrt{a^2 - b^2}}{ab} \right) & 0\\ 0 & \frac{\dot{b}}{b} & 0\\ 0 & 0 & \frac{\dot{c}}{c} \end{bmatrix}$$
(42)

At this point, it is straightforward to compute stress power in the deformed configuration ( $\sigma : \mathbf{D} = \sigma : \mathbf{L}$ ). The local form in the deformed configuration as given in Eq. (16) thus becomes

$$\frac{d\psi}{dt} - \frac{\mathbf{\sigma}}{\rho} : \mathbf{D} = \frac{d\psi}{dt} - \frac{F}{\rho(abc)} \left( \frac{a\dot{a} - b\dot{b}}{\sqrt{a^2 - b^2}} - \frac{\dot{a}\sqrt{a^2 - b^2}}{a} \right) \le 0 \tag{43}$$

where F is the force acting on the shearing surface  $(X_2 = 1)$ . From the conservation of mass equation,  $\rho(abc) = \rho J = \rho_0$ , where J is the determinant of tensor  $\mathbf{F}$ . Therefore, in the reference configuration, Eq. (43) is written as

$$\frac{d\psi}{dt} - \frac{T_{21}}{\rho_0} \left(\frac{\dot{a}b - a\dot{b}}{\sqrt{a^2 - b^2}}\right) \le 0 \tag{44}$$

where  $T_{21} = F/A_0$  (where  $A_0 = 1$ ) is the 2-1 component of tensor  $T_0$ . The nominal shear strain  $\gamma$  can be related to a and b

$$\gamma = \frac{d}{b} = \sqrt{\left(\frac{a^2}{b^2} - 1\right)} \tag{45}$$

It is worth noting that unlike the simple shear condition where a single parameter  $\gamma$  completely characterizes the strain state, two independent deformation parameters (any two out of a, b and  $\gamma$ ) are required to describe the deformation state in pure shear. The *specific energy input*  $\Pi$  is thus a function whose time derivative is the second term in Eq. (44), that is, the specific thermodynamic *stress power* is given by

$$\frac{d\Pi}{dt} = \frac{\partial\Pi}{\partial a}\dot{a} + \frac{\partial\Pi}{\partial b}\dot{b} = \frac{T_{21}}{\rho_0} \left( \left( \frac{b^2}{a\sqrt{a^2 - b^2}} \right) \dot{a} + \left( \frac{-b}{\sqrt{a^2 - b^2}} \right) \dot{b} \right) \tag{46}$$

Eq. (46) shows that in pure shear, the expression for stress power can be decomposed into linear components related to the rate of change of independent dimensions a and b. The specific energy input corresponding to an individual dimensional rate (a or b) is given by the partial derivative with respect to that dimension. Two extreme cases in this context can be those in which one dimension is kept constant and the energy input owes to the change in a single dimension (for a certain shear strain value (Eq. (45))). The rate of change of available energy for these cases can be given in terms of the shear strain  $\gamma$ ,

$$\frac{d\phi_{PS}}{dt}\bigg|_{\dot{a}=0} = \frac{d}{dt}\left(\rho_0\psi - \frac{T_{21}\gamma}{\sqrt{1+\gamma^2}}\right) \le 0; \qquad \frac{d\phi_{PS}}{dt}\bigg|_{\dot{b}=0} = \frac{d}{dt}\left(\rho_0\psi - T_{21}\tan^{-1}\gamma\right) \le 0 \tag{47}$$

where the subscript PS indicates pure shear deformation mode. The thermodynamic stability criterion can now be given as

$$\frac{d\phi_{PS}(\gamma)}{d\gamma} = 0, \quad \frac{d^2\phi_{PS}(\gamma)}{d\gamma^2} > 0 \tag{48}$$

By substituting individual rates of change of available energy given in Eq. (47) into Eq. (48), the stability criteria in terms of the free energy function  $\psi$  becomes

$$\frac{d\phi_{PS}(\gamma)}{d\gamma}\bigg|_{\dot{a}=0} = \frac{d\psi}{d\gamma} - \frac{T_{21}}{\rho_0(1+\gamma^2)^{3/2}} = 0; \qquad \frac{d\phi_{PS}(\gamma)}{d\gamma}\bigg|_{\dot{b}=0} = \frac{d\psi}{d\gamma} - \frac{T_{21}}{\rho_0(1+\gamma^2)} = 0 \tag{49a}$$

$$\frac{d^2\phi_{PS}(\gamma)}{d\gamma^2}\bigg|_{\dot{a}=0} = \frac{d^2\psi}{d\gamma^2} + \frac{3\gamma}{\left(1+\gamma^2\right)}\frac{d\psi}{d\gamma} > 0; \qquad \frac{d^2\phi_{PS}(\gamma)}{d\gamma^2}\bigg|_{\dot{b}=0} = \frac{d^2\psi}{d\gamma^2} + \frac{2\gamma}{\left(1+\gamma^2\right)}\frac{d\psi}{d\gamma} > 0 \tag{49b}$$

To determine the polynomial form of Helmholtz free energy function  $\psi$ , the tensor  $\mathbf{C}$  and its principal invariants are written as

$$\mathbf{C}|_{\dot{a}=0} = \begin{bmatrix} 1 & \frac{\gamma}{\sqrt{1+\gamma^2}} & 0\\ \frac{\gamma}{\sqrt{1+\gamma^2}} & 1 & 0\\ 0 & 0 & 1+\gamma^2 \end{bmatrix}, \quad I_1|_{\dot{a}=0} = \gamma^2 + 3, \quad I_2|_{\dot{a}=0} = \frac{\gamma^2 (1+2\gamma^2)}{1+\gamma^2} + 3$$
 (50a)

$$\mathbf{C}|_{\dot{b}=0} = \begin{bmatrix} 1+\gamma^2 & \gamma\sqrt{1+\gamma^2} & 0\\ \gamma\sqrt{1+\gamma^2} & 1+\gamma^2 & 0\\ 0 & 0 & \frac{1}{1+\gamma^2} \end{bmatrix}, \quad I_1|_{\dot{b}=0} = \frac{\gamma^2(1+2\gamma^2)}{1+\gamma^2} + 3, \quad I_2|_{\dot{b}=0} = \gamma^2 + 3$$
 (50b)

Note that the first and second invariants of **C** in Eq. (50a) are the second and first invariants in Eq. (50b), respectively. When plotted as a function of  $\gamma$ , the two invariant functions differ by less than five percent at shear strains as large as 0.2. Using these invariants, the nominal shear stresses can be determined using Eq. (49a) for the two extreme cases,  $\dot{a}=0$  and  $\dot{b}=0$  (the two deformations that can independently affect  $\gamma$ ). Finally, the thermodynamic stability criterion for a given limiting shear strain  $\gamma$  is determined using the intersection of the inequalities in Eq. (49b).

Using Eqs. (20), (49a) and (49b), the nominal shear stress  $T_{21}$  is

$$T_{21}|_{\dot{a}=0} = \left(1+\gamma^{2}\right)^{\frac{3}{2}} \left\{ 2\rho_{0}\psi_{10}\gamma + 2\rho_{0}\psi_{01}\gamma \frac{\left(2\gamma^{4}+4\gamma^{2}+1\right)}{\left(1+\gamma^{2}\right)^{2}} + 2\rho_{0}\psi_{11}\gamma^{3} \frac{\left(4\gamma^{4}+7\gamma^{2}+2\right)}{\left(1+\gamma^{2}\right)^{2}} + \mathcal{O}\left((I_{1}-3)^{2}, (I_{2}-3)^{2}\right) \right\}$$

$$(51a)$$

$$T_{21}|_{\dot{b}=0} = \left(1 + \gamma^{2}\right) \left\{ 2\rho_{0}\psi_{10}\gamma \frac{\left(2\gamma^{4} + 4\gamma^{2} + 1\right)}{\left(1 + \gamma^{2}\right)^{2}} + 2\rho_{0}\psi_{01}\gamma + 2\rho_{0}\psi_{11}\gamma^{3} \frac{\left(4\gamma^{4} + 7\gamma^{2} + 2\right)}{\left(1 + \gamma^{2}\right)^{2}} + \mathcal{O}\left((I_{1} - 3)^{2}, (I_{2} - 3)^{2}\right) \right\}$$

$$(51b)$$

Using the stability conditions in Eq. (49b) and the material parameters in Eq. (23),

$$\frac{d^{2}\phi_{PS}(\gamma)}{d\gamma^{2}}\Big|_{\dot{a}=0} = 2A_{10}\left(\frac{1+4\gamma^{2}}{1+\gamma^{2}}\right) + 2A_{01}\frac{\left(8\gamma^{6}+18\gamma^{4}+12\gamma^{2}+1\right)}{\left(1+\gamma^{2}\right)^{3}} + 2A_{11}\gamma^{2}\frac{\left(24\gamma^{6}+56\gamma^{4}+39\gamma^{2}+6\right)}{\left(1+\gamma^{2}\right)^{3}} + \mathcal{O}\left((I_{1}-3)^{2},(I_{2}-3)^{2}\right) > 0$$
(52a)

$$\frac{d^{2}\phi_{PS}(\gamma)}{d\gamma^{2}}\bigg|_{\dot{b}=0} = 2A_{10} \frac{\left(6\gamma^{6} + 14\gamma^{4} + 11\gamma^{2} + 1\right)}{\left(1 + \gamma^{2}\right)^{3}} + 2A_{01} \left(\frac{1 + 3\gamma^{2}}{1 + \gamma^{2}}\right) + 2A_{11}\gamma^{2} \frac{\left(20\gamma^{6} + 49\gamma^{4} + 37\gamma^{2} + 6\right)}{\left(1 + \gamma^{2}\right)^{3}} + \mathcal{O}\left((I_{1} - 3)^{2}, (I_{2} - 3)^{2}\right) > 0$$
(52b)

which are the two T-C inequalities whose intersection determines the ROS of a polynomial hyperelastic model under pure shear.

## 3.4. Coefficient functions of the generalized thermodynamic constitutive (T-C) inequality

As shown in Eq. (24), the generalized form of the T-C inequality for polynomial hyperelastic models can be expressed in terms of the summation of the products of individual model constants with a strain-dependent coefficient function  $\zeta_{mn}(\varepsilon)$ . Individual coefficient functions for primary deformation modes are thus obtained by comparing their T-C inequality (Eqs. (31), (37) and (52) for uniaxial, simple shear and pure shear, respectively) with Eq. (24), and are summarized in Table 1.

**Table 1** Strain-dependent coefficients  $\zeta_{mn}(\varepsilon)$  in the generalized T-C inequality (Eq. (24)) for various deformation modes.

Deformation mode	ζ 10	ζ01	ζ 11
Uniaxial (compression and tension)	$2\left(1+\frac{2}{\lambda^3}\right)$	$\frac{6}{\lambda^4}$	$6\left(2\lambda-1+\frac{4}{\lambda^5}-\frac{3}{\lambda^4}-\frac{2}{\lambda^3}\right)$
Simple shear	2	2	$12\gamma^2$
Pure shear	$\frac{2 (6\gamma^6 + 14\gamma^4 + 11\gamma^2 + 1)}{(1+\gamma^2)^3}$	$2(\frac{1+3\gamma^2}{1+\gamma^2})$	$\frac{2\dot{\gamma}^2(20\gamma^6 + 49\gamma^4 + 37\gamma^2 + 6)}{(1+\gamma^2)^3}$
ruic siicai	$2\left(\frac{1+4\gamma^2}{1+\gamma^2}\right)$	$\frac{2 (6\gamma^6 + 14\gamma^4 + 11\gamma^2 + 1)}{(1 + \gamma^2)^3}$	$\frac{2\gamma^{2}(24\gamma^{6} + 56\gamma^{4} + 39\gamma^{2} + 6)}{(1+\gamma^{2})^{3}}$

#### 4. Constitutive inequalities for common polynomial hyperelastic models

In this section, constitutive inequalities for three common polynomial models, namely, the neo-Hookean model, the two-parameter Mooney-Rivlin model (based on Mooney, 1940; Rivlin, 1948b), and the three-parameter generalized Rivlin model, are determined using the general T-C inequalities derived in Section 3. These models are *ab initio* consistent with both the linear and the weakly nonlinear theory of elasticity (Hamilton et al., 2004), which is a minimal requirement generally imposed in order to capture nonlinear effects (Destrade et al., 2017, 2010). The thermodynamic inequalities derived are compared with the adscititious Baker-Ericksen (B-E) and E-inequalities for the respective models and deformation modes.

## 4.1. Neo-Hookean model

The neo-Hookean (NH) model is the simplest of all polynomial hyperelastic models. The strain energy density in the NH model is linearly dependent on a single hyperelastic model constant as

$$W = A_{10}(I_1 - 3) \tag{53}$$

Unlike higher order polynomial models such as Mooney Rivlin and three-parameter generalized Rivlin models, which are phenomenological in nature, the NH model is a micromechanical model, which can be derived from the molecular theory of rubber-like networks (Treloar, 1943). The model constant  $A_{10}$  is given by

$$2A_{10} = N_p k\theta \tag{54}$$

where  $A_{10}$  is the NH model constant,  $N_p$  is the density of polymer chains, k is the Boltzmann constant, and  $\theta$  is the absolute temperature.

Using the general T-C inequality (Eq. (24)) and the first-order coefficients ( $\zeta_{10}$ ) from Table 1, constitutive inequalities for the various primary deformation modes in an NH material under compression, tension, simple shear or pure shear, are given as

$$A_{10} > 0 \tag{55}$$

Note, although the T-C inequalities for uniaxial deformation and pure shear cases in an NH material are  $A_{10}(1+2/\lambda^3)>0$  and  $A_{10}(1+4\gamma^2/1+\gamma^2)>0$ ,  $A_{10}(6\gamma^6+14\gamma^4+11\gamma^2+1)/(1+\gamma^2)^3>0$ , respectively, the  $\zeta_{10}(\epsilon)$  in these cases are always positive regardless of the limiting strain (strain at maximum stress) in the material. Thus, the constitutive inequality is independent of the stretch or strain, and can be simplified as Eq. (55).

In order to compare the thermodynamic inequality given by Eq. (55) with the adscititious inequalities, it is important to find a relation between the response functions in Eq. (2) and the NH model constant in Eq. (53). To this end, the hyperelastic Cauchy stress tensor  $\sigma$  is determined by transforming the second Piola-Kirchhoff tensor  $\mathbf{S}$  in the deformed configuration, and then comparing that with Eq. (2) as

$$\boldsymbol{\sigma} = -p\mathbf{1} + 2\frac{\partial W}{\partial \mathbf{B}}\mathbf{B} = s_0\mathbf{1} + s_1\mathbf{B} + s_2\mathbf{B}^{-1}$$
(56)

where p is the Lagrange multiplier pertaining to the incompressibility constraint. Using Eqs. (53) and (56), the response functions and model constants for an NH incompressible material are related as

$$s_0 = -p, \ s_1 = 2A_{10}, \ s_2 = 0$$
 (57)

Using Eqs. (57), (5) and (7), the adscititious inequalities for an NH constitutive model under incompressibility can be written as

B-E or E 
$$A_{10} > 0$$
 (58)

Thus, regardless of the limiting strain or deformation mode, the limit on  $A_{10}$  in an NH material is such that it must always be greater than zero. The ROS for the NH model is thus a 1-D ray that starts from  $A_{10} = 0$  and extends toward positive infinity (excludes  $A_{10} = 0$ ). In addition, for the NH model, the T-C inequalities for primary deformation modes are identical to the adscititious B-E and E-inequalities,

$$T-C_{U.SS,PS} \Leftrightarrow B-E \Leftrightarrow E$$
 (59)

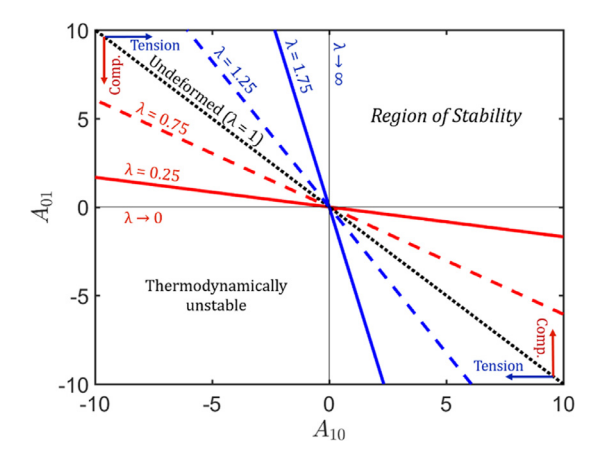


**Fig. 4.** Region of stability for the Mooney-Rivlin model under uniaxial deformation mode. The ROS of model constants in infinitesimal strain conditions is defined by the  $\lambda = 1$  line. The ROS in finite limiting strain condition is obtained by the intersection of small strain stability region and the region defined by the T-C inequality under that limiting strain value (in compression or tension).

where subscripts U, SS and PS represent, respectively, the uniaxial deformation, simple shear and pure shear states, and the symbol  $\Leftrightarrow$  denotes logical equivalence.

As the stability criterion for the NH model is independent of the primary deformation mode considered in the experiment, the obtained model constant will always be thermodynamically stable (or feasible). In other words, even if the NH material constant obtained from one deformation mode test may not be able to accurately fit experimental data for another deformation mode, only a single experiment is theoretically sufficient to yield a thermodynamically stable model constant.

#### 4.2. Mooney-Rivlin model

The Mooney-Rivlin (MR) model is a two-parameter hyperelastic model bilinear with respect to the non-zero principal invariants of tensor  $\mathbf{C}$ ,

$$W = A_{10}(I_1 - 3) + A_{01}(I_2 - 3)$$
(60)

The T-C inequalities for the MR model depend both on the deformation mode and on limiting strains. The following subsections analyze the ROS for each primary deformation mode separately.

## 4.2.1. Uniaxial deformation (compression or tension)

The ROS for the MR model in uniaxial deformation can be determined by using the first two terms in Eq. (31) and the coefficients from Table 1, as

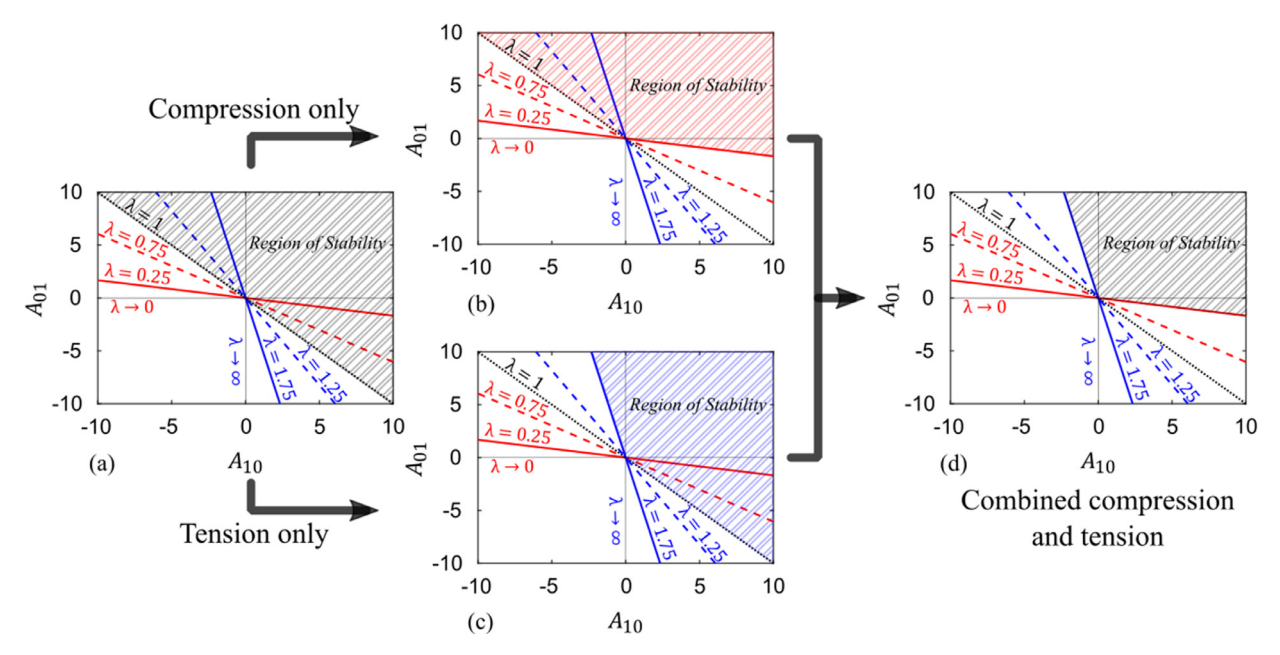
$$2A_{10}\left(1+\frac{2}{\lambda^3}\right) + A_{01}\left(\frac{6}{\lambda^4}\right) > 0 \tag{61}$$

Fig. 4 shows the ROS for the MR model under various limiting strains for uniaxial deformation where  $A_{10}$  and  $A_{01}$  are on the x-axis and y-axis, respectively. In this plot, the line  $A_{10} + A_{01} = 0$  refers to the initial undeformed state  $(\lambda = 1)$ ,  $A_{01} = 0$  to infinite compression  $(\lambda \to 0)$ , and  $A_{10} = 0$  to infinite tension  $(\lambda \to \infty)$ . Unlike the one-dimensional NH ROS, for the two-parameter MR model, ROS is a two-dimensional open half-space that is a function of both the deformation mode and stretch/strain limits. Fig. 5 illustrates the evolution of the ROS from small to large stretch limit cases in uniaxial deformation. Note that for experiments involving infinitesimally small deformations, regardless of the mode of uniaxial deformation (i.e., compression or tension), the actual limits on material parameters are dictated by the inequality given as  $A_{10} + A_{01} > 0$  (hatched portion in Fig. 5(a)). Under this condition, the entire half-plane to the right of  $\lambda = 1$  line is the ROS, and material parameters can take any value in this region. However, for finite strain tests under tension or compression, the feasible region for hyperelastic model constants becomes smaller.

For example, consider a situation when only a compression test is conducted to characterize material behavior using the MR model. For any finite compression stretch limit  $\lambda_L$ , the ROS will be a smaller region than that under the small strain condition (Fig. 5(b)), and the space reduction will be on the fourth quadrant ( $A_{10} > 0$ ,  $A_{01} < 0$ ). As  $\lambda_L \to 0$ , the material parameter limit will take the form given by

$$A_{10} + A_{01} > 0, \quad A_{01} \ge 0$$
 (62)

Similarly, when only a tension test is performed to obtain MR model parameters, the ROS will again be smaller than that under the small strain condition. However, unlike the compression case, the reduction in the ROS will occur in the second



**Fig. 5.** Evolution of the *Region of stability* with uniaxial deformation in MR model. (a) For small compressive and/or tensile deformation  $(A_{10} + A_{01} > 0)$ , (b) for compression test data only with limiting stretch  $\lambda = 0.25$  (engineering strain  $\varepsilon = -0.75$ ), (c) for tensile test data only with limiting stretch  $\lambda = 1.75$  ( $\varepsilon = 0.75$ ), and (d) for combined compression and tension tests with material stretch (or strain) limits  $\lambda = 0.25$  and  $\lambda = 1.75$  (or  $\varepsilon = \pm 0.75$ ).

quadrant  $(A_{10} < 0, A_{01} > 0)$  as shown in Fig. 5(c). For a material that can be infinitely deformed under tension, the material parameter limits will take the form given by

$$A_{10} + A_{01} > 0, \quad A_{10} \ge 0$$
 (63)

As the area deducted from the initial ROS by individual compression and tension deformation does not overlap for any finite strain, material parameters obtained using a single deformation mode test may not be stable or feasible for another deformation mode. Thus, it can be concluded that both compression and tension experiments should be conducted to ensure the thermodynamic stability of MR parameters. Fig. 5(d) shows the ROS under combined compression ( $\lambda_L = 0.25$ ) and tension ( $\lambda_L = 1.75$ ) experiments. Obviously, for a material that can undergo infinite hyperelastic stretch in tension, and infinite compressibility in compression, the ROS converges to the first quadrant ( $A_{10} > 0$ ,  $A_{01} > 0$ ).

The response functions in Eq. (2) can be written in terms of MR model constants using Eq. (56) as

$$s_0 = -p, \quad s_1 = 2A_{10}, \quad s_2 = -2A_{01}$$
 (64)

Using Eqs. (64), (5) and (7), the adscititious inequalities for the MR constitutive model under uniaxial deformation are given as

B-E: 
$$A_{10} + \frac{A_{01}}{\lambda} > 0$$
 (65)

E: 
$$A_{10} > 0$$
,  $A_{01} > 0$  (66)

The stability region given by E-inequalities (Eq. (66)) is the first quadrant of the  $A_{10}$  versus  $A_{01}$  plot as shown in Fig. 4. For a material that has a finite limit of strain in compression and tension (Fig. 5(d)), this region is always a subset of the ROS given by the T-C inequality (Eq. (61)). In other words, if the E-inequalities hold true, then the T-C inequalities necessarily do so. However, in case the E-inequalities are not satisfied, nothing can be said about the T-C inequalities. Thus, it can be concluded that the E-inequality implies the T-C inequality, but the reverse is not true.

To compare the T-C and B-E inequalities, one possible approach would be to compare slopes of the  $A_{10}$  versus  $A_{01}$  plot constructed using these inequalities (i.e. slope of the line obtained by replacing the inequality with an equality) at a given limiting strain (e.g., Fig. 4 for the T-C inequality). Mathematically, using Eqs. (61) and (65),

$$m_{T-C}(\lambda) = \left(\frac{A_{01}}{A_{10}}\right)_{T-C} = \frac{-1}{3}(\lambda^4 + 2\lambda); \quad m_{B-E}(\lambda) = \left(\frac{A_{01}}{A_{10}}\right)_{B-E} = -\lambda$$
 (67)

where m denotes the slope, and subscripts T-C and B-E represent the thermodynamic constitutive and the Baker-Ericksen inequalities, respectively.

Fig. 6 plots the slope  $m = A_{01}/A_{10}$  as obtained in Eq. (67) for T-C and B-E inequalities as a function of uniaxial stretch  $\lambda$ . As described in the preceding paragraphs, the inequality that leads to a smaller magnitude slope in the  $A_{10}$  versus  $A_{01}$  plot for

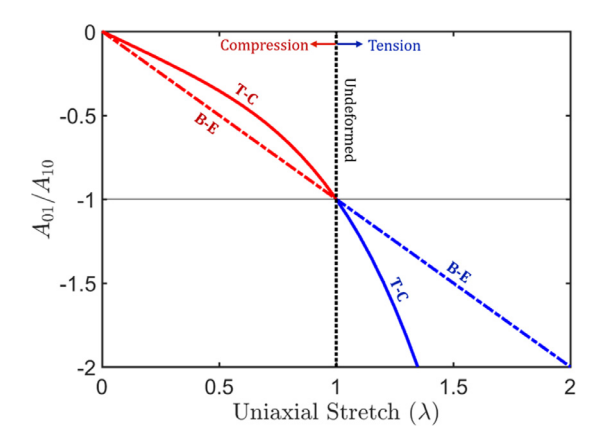


**Fig. 6.**  $(A_{01}/A_{10})$  versus uniaxial stretch plot for B-E and T-C inequalities.

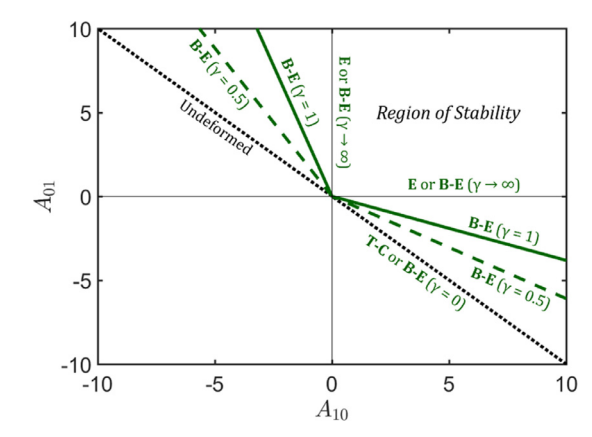


Fig. 7. Comparison of the Region of stability (2-D) of T-C inequality under simple shear with B-E and E-inequalities.

compression state is a more conservative (smaller ROS) constitutive inequality. Similarly, for a tension state, the inequality that yields a greater magnitude slope in the  $A_{10}$  versus  $A_{01}$  plot is more conservative. From Fig. 6, it can be seen that the slope of the T-C inequality is always smaller in magnitude in compression and greater in magnitude in tension. Therefore, it can be concluded that regardless of the material limiting strain, the B-E inequality is always implied by the T-C inequality in uniaxial deformation, but not vice versa. Thus, in theory, while E-inequalities are excessively stringent, B-E inequality on the other hand is excessively lenient and may allow thermodynamically unstable model constants (especially in tension where slopes are diverging (Fig. 6)). Thus, for the MR model,

$$E \Rightarrow T - C_{IJ} \Rightarrow B - E \tag{68}$$

where symbol  $\Rightarrow$  denotes logical implication.

#### 4.2.2. Simple. shear

The thermodynamic stability of an MR material in simple shear is defined by the T-C inequality given by

$$A_{10} + A_{01} > 0 ag{69}$$

Eq. (69) is identical to the small strain thermodynamic stability condition for uniaxial deformation mode ( $\lambda = 1$  line in Fig. 4). To define the B-E inequalities for simple shear, the eigenvalues of  $\mathbf{C}$  (Eq. (34)) are computed and then substituted in Eq. (5), resulting in three different inequalities (no two principal stretches are equal). The stable region for model constants is the intersection of the half-planes yielded by individual inequalities.

B-E: 
$$A_{10} + A_{01} > 0, \quad A_{10} + \frac{A_{01}}{\left(1 + \frac{\gamma^2}{2}\right) \pm \frac{\gamma\sqrt{\gamma^2 + 4}}{2}} > 0$$
 (70)

E: 
$$A_{10} > 0, \quad A_{01} \ge 0$$
 (71)

From Eqs. (69), (70) and (71), it is clear that the B-E inequality is the only condition in simple shear deformation of an MR material that is dependent on limiting shear strain. Fig. 7 compares the three inequalities based on the region of

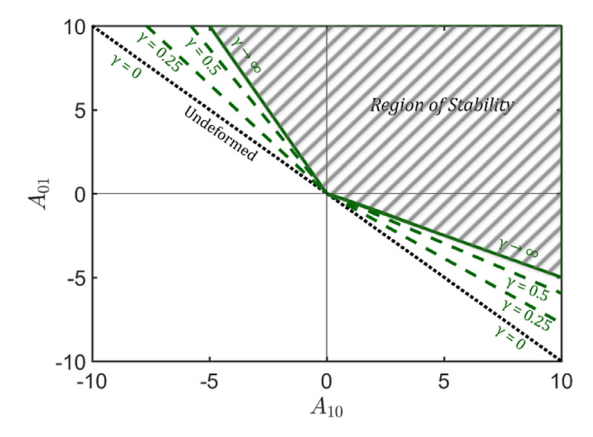


Fig. 8. Region of stability (2-D) for the Mooney-Rivlin model under pure shear. Hatched region represents the smallest ROS, which is obtained when  $\gamma \to \infty$ .

allowed stable parameters. It can be seen that the T-C inequality results in an ROS that is the entire region to the right of the "Undeformed" line. The E-inequality, on the other hand, allows only positive model constants, and can be represented as the first quadrant of the above plot. The B-E inequality, which is a function of the limiting shear strain, results in a stable region that is smaller than that yielded by the T-C inequality, but larger than the E-inequality region. Furthermore, for the infinitesimally small strain case ( $\gamma \to 0$ ), the B-E inequality is identical to the T-C inequality (see Fig. 7). As the limiting shear strain tends to infinity, the B-E inequality converges to the E-inequalities.

Thus, for simple shear deformation in the MR model, the T-C inequality is implied by B-E inequalities, and the B-E inequalities are implied by E-inequalities. In either of these implications, the reverse relation is not necessarily true. For the MR model,

$$E \Rightarrow B-E \Rightarrow T-C_{SS} \tag{72}$$

#### 4.2.3. Pure shear

Using coefficients from Table 1, the stability of an MR material in pure shear is defined by T-C inequalities,

$$A_{10}\left(\frac{1+4\gamma^{2}}{1+\gamma^{2}}\right) + A_{01}\frac{\left(8\gamma^{6} + 18\gamma^{4} + 12\gamma^{2} + 1\right)}{\left(1+\gamma^{2}\right)^{3}} > 0,$$

$$A_{10}\frac{\left(6\gamma^{6} + 14\gamma^{4} + 11\gamma^{2} + 1\right)}{\left(1+\gamma^{2}\right)^{3}} + A_{01}\left(\frac{1+3\gamma^{2}}{1+\gamma^{2}}\right) > 0$$

$$(73)$$

Fig. 8 shows the plot of the ROS for the MR model under pure shear deformation. Under small strains, the stability is governed by the inequality  $A_{10} + A_{01} > 0$  as defined by the  $\gamma = 0$  line in the plot. As the material limiting strain increases, the first and second inequalities in Eq. (73) reduce the size of the ROS in the fourth and second quadrant, respectively. At infinite limiting strains, the ROS achieves its minimum size and can be represented by the intersection of the half-planes created by the  $\gamma = 0$  line and the solid lines corresponding to  $\gamma \to \infty$  (hatched region in Fig. 8). This behavior is different from that in the uniaxial deformation case where the ROS finally converged to the one dictated by the E-inequalities (first quadrant).

It can be concluded that regardless of the material limiting strain, a definite inequality can be defined for the MR model constants under pure shear. By taking the limit of Eq. (73) as  $\gamma \to \infty$ ,

$$T-C_{PS-\infty}$$
:  $A_{10} + 2A_{01} > 0$ ,  $2A_{10} + A_{01} > 0$  (74)

where subscript  $PS-\infty$  represents that the ROS defined by this inequality is for a hypothetical pure shear situation when the limiting shear strain tends to infinity. In terms of the initial shear modulus G, which can be obtained by small strain experiments,

$$T-C_{PS-\infty}$$
:  $A_{10}, A_{01} \in \left(-\frac{G}{2}, G\right)$  (75)

where G is a model independent material constant, and is written in terms of the model constants of an MR (or the three-parameter generalized Rivlin) model as

$$G = 2(A_{10} + A_{01}) \tag{76}$$

To define the B-E inequalities for this case, the eigenvalues of C (Eq. (50b)) are computed and then substituted in Eq. (5), again resulting in three different inequalities,

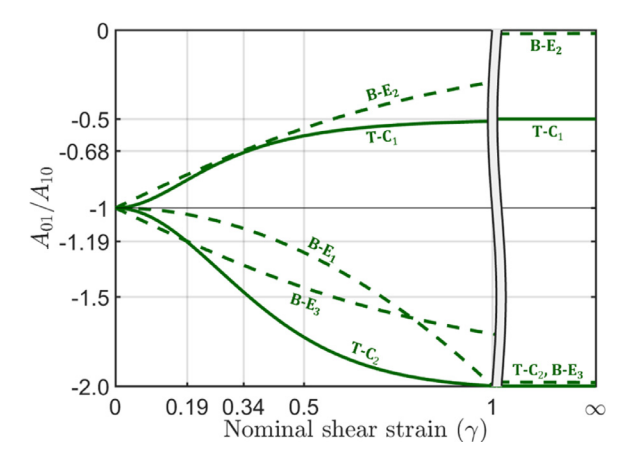


**Fig. 9.**  $(A_{01}/A_{10})$  versus nominal shear strain plot for B-E and T-C inequalities.

B-E: 
$$A_{10} + \frac{A_{01}}{\gamma^2 + 1} > 0, \quad A_{10} + \frac{A_{01}}{\left(1 \mp \frac{\gamma}{\sqrt{\gamma^2 + 1}}\right)} > 0$$
 (77)

E: 
$$A_{10} > 0, \quad A_{01} \ge 0$$
 (78)

To compare Eq. (73) with the B-E inequalities, the slopes of the  $A_{10}$  versus  $A_{01}$  plot obtained using these inequalities (i.e., slope of the line obtained by replacing the inequality with an equality) at a given limiting strain is compared with those obtained using the T-C inequalities Eq. (73)). By using Eqs. (73) and (77),

$$m_{T-C}^{1}(\gamma) = \frac{-\left(1+\gamma^{2}\right)^{2}\left(1+4\gamma^{2}\right)}{\left(8\gamma^{6}+18\gamma^{4}+12\gamma^{2}+1\right)}, \quad m_{T-C}^{2}(\gamma) = \frac{-\left(6\gamma^{6}+14\gamma^{4}+11\gamma^{2}+1\right)}{\left(1+\gamma^{2}\right)^{2}\left(1+3\gamma^{2}\right)}$$
(79a)

$$m_{\mathrm{B-E}}^{1}(\gamma) = -(\gamma^{2} + 1), \quad m_{\mathrm{B-E}}^{2,3}(\gamma) = -1 \pm \frac{\gamma}{\sqrt{\gamma^{2} + 1}}$$
 (79b)

where m denotes the slope, with subscripts T-C and B-E representing the corresponding inequalities, and superscripts denoting their respective equation numbers as they appear in Eqs. (73) and (77).

Fig. 9 shows the plot of the slope equations given in Eq. (79) versus nominal shear strain  $\gamma$ , where the solid lines represent the two T-C inequalities (T-C<sub>1</sub> and T-C<sub>2</sub> corresponds to the first and second inequalities in Eq. (73)), and the broken lines denote the three B-E inequalities (B-E<sub>1</sub>, B-E<sub>2</sub> and B-E<sub>3</sub> represent the three inequalities in Eq. (77)). The two inequalities (T-C and B-E) are equivalent under small strain condition, which corresponds to  $\gamma = 0$  ( $A_{01}/A_{10} = -1$ ) in the figure. As the limiting shear strain increases, the slope lines corresponding to the T-C and B-E inequalities diverge with respect to the line  $A_{01}/A_{10} = -1$ , causing their corresponding intersected stability regions to become progressively smaller. While the T-C<sub>1</sub> and B-E<sub>2</sub> inequalities reduce the size of their respective stability regions in the fourth quadrant of the  $A_{10}-A_{01}$  plot (Fig. 8), inequalities T-C<sub>2</sub>, B-E<sub>1</sub> and B-E<sub>3</sub> reduce the size in the second quadrant ( $A_{01} > 0$ ,  $A_{10} < 0$ ). At extreme values of shear strain ( $\gamma \to \infty$ ), the ROS defined by the T-C inequalities attains its minimum as given in Eq. (74). Under such conditions, while the first and second B-E inequalities converge to the first and second E-inequalities, respectively, the third B-E inequality becomes  $2A_{10} + A_{01} > 0$ .

At any arbitrary limiting shear strain value, the slope of the  $T-C_1$  inequality is greater in magnitude as compared to the second B-E inequality ( $T-C_1$  and  $B-E_2$  define ROS reduction in the fourth quadrant of the  $A_{10}-A_{01}$  plot), making it a more conservative inequality in the fourth quadrant. However, there is no such definitive relation between  $T-C_2$  and the other two B-E inequalities, which define the ROS in the second quadrant as evident from their multiple intersections (between lines  $T-C_2$  and  $T-C_2$  and  $T-C_3$  and  $T-C_4$  and  $T-C_5$  and  $T-C_5$  and  $T-C_6$  and

$$E \Rightarrow B-E, \quad E \Rightarrow T-C_{PS}$$
 (80)

Furthermore, considering strain independent general inequalities given in Eqs. (74) and (78), for a hypothetical material that fails at  $\nu \to \infty$ ,

$$E \Leftrightarrow B-E_{PS-\infty} \Rightarrow T-C_{PS-\infty}$$
 (81)

where subscript  $PS-\infty$  represents pure shear at infinite limiting shear strain.

Note that unlike the NH model in which constitutive inequalities are independent of the deformation mode and limiting strain values, the MR model presents a more complex situation where limits on model constants are not only a function

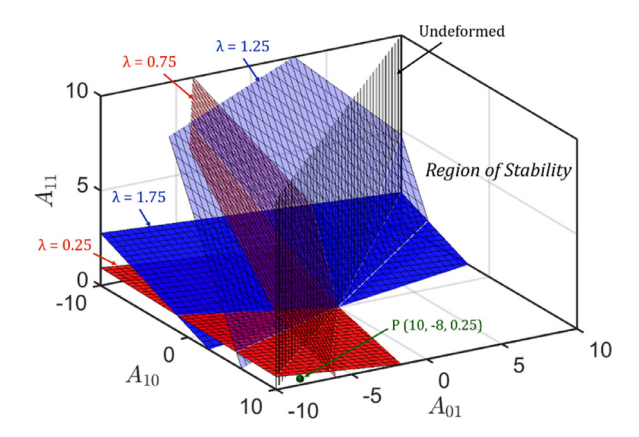


Fig. 10. Region of Stability (3-D) for the generalized Rivlin model under uniaxial deformation.

of limiting strain, but also the deformation mode under consideration. On one hand, for materials that remain hyperelastic only in the infinitesimally small strain regime, the limits on model constants can be defined by the inequality  $A_{10} + A_{01} > 0$ . On the other hand, for a material that can undergo extreme deformations, inequalities  $A_{10} > 0$  and  $A_{01} > 0$  define the bounds. Many materials such as biological tissues and hydrogels, however, remain hyperelastic until a finite moderate strain limit. The choice of experiment(s) to obtain hyperelastic model constants in such materials thus affects not only the accuracy of the model to describe a complex three-dimensional stress state, but also the thermodynamic stability of the model constants so obtained. As described in Section 4.2.1, it is possible that the model constants obtained from one type of uniaxial deformation experiment (e.g., compression) are thermodynamically unreasonable to describe the other deformation mode (tension). Moreover, although simple shear deformation requires a limiting strain independent T-C inequality, the model constants must follow Eq. (73) to be thermodynamically stable to describe pure shear. As compression, tension and shear are the primary deformation modes, it can be concluded that for a material having arbitrary finite limiting strains, all primary deformation experiments must be conducted to be certain that the model constants so obtained are thermodynamically stable in a three-dimensional sense.

#### 4.3. Three-parameter generalized Rivlin model

The three-parameter generalized Rivlin (GR) model has a bilinear form of W,

$$W = A_{10}(I_1 - 3) + A_{01}(I_2 - 3) + A_{11}(I_1 - 3)(I_2 - 3)$$
(82)

Although inclusion of a third model constant  $A_{11}$  makes this model more versatile and accurate for complex nonlinear stress-strain responses (Kumar and Rao, 2016), it also adds complexity in the determination of parameters and their respective bounds. Similar to the MR model, the T-C inequalities for the GR model depend on both the deformation mode and the limiting strains. The following subsections analyze each deformation mode separately.

#### 4.3.1. Uniaxial deformation (compression or tension)

When a uniaxial deformation is modeled using the GR model, the thermodynamic stability criterion (Eq. (31)) takes the form of the T-C inequality as

$$A_{10}\left(1+\frac{2}{\lambda^3}\right) + A_{01}\left(\frac{3}{\lambda^4}\right) + 3A_{11}\left(2\lambda - 1 + \frac{4}{\lambda^5} - \frac{3}{\lambda^4} - \frac{2}{\lambda^3}\right) > 0 \tag{83}$$

Unlike the MR model ROS, which is a two-dimensional half-plane, the ROS for three-parameter polynomial hyperelastic models are three-dimensional open half-spaces. Fig. 10 shows the ROS for the GR model under uniaxial deformation. Under infinitesimal strain conditions, the ROS is defined by the inequality given as  $A_{10} + A_{01} > 0$ . This is represented by the region in front of the "Undeformed" plane toward the first octant ( $A_{01} > 0$ ,  $A_{10} > 0$ ,  $A_{11} > 0$ ), where  $A_{11}$  is totally unrestrained and can take any real value. However, for materials with a finite limiting strain in compression and tension, the ROS reduces in size. As shown in the figure, the planes defining the ROS tilt toward the  $A_{10}$ - $A_{01}$  plane ( $A_{11} = 0$ ), becoming completely level (parallel) on this plane as limiting stretch in compression and tension tends to zero and infinity, respectively. Mathematically, for a hyperelastic material that can sustain infinite tensile and compressive strains, the necessary but not sufficient condition for thermodynamic stability is

$$T-C_{11-\infty}^*$$
:  $A_{10}+A_{01}>0$ ,  $A_{11}>0$  (84)

where the subscript  $U-\infty$  represents infinite uniaxial deformation (compression or tension) and the superscript \* denotes that this is not a sufficient condition (and may fail).

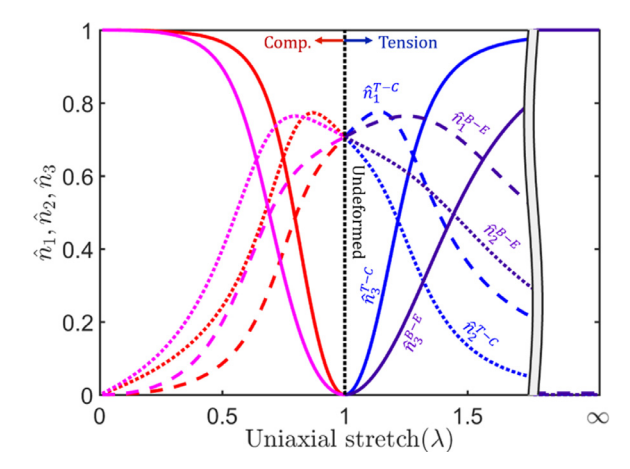


Fig. 11. Comparison of unit normal components of planes defined by B-E and T-C hyperplanes as a function of uniaxial stretch.

Note that Eq. (84) is not the sufficient condition for stability. For example, although the set of model constants corresponding to the point  $\{A_{10}, A_{01}, A_{11}\} = \{10, -8, 0.25\}$  follow Eq. (84), they are thermodynamically unstable when the limiting strain of a material in compression is  $\lambda = 0.75$  (also at  $\lambda = 0.25$ ) (see point P in Fig. 10). Furthermore, the material parameters obtained using only one uniaxial deformation mode may or may not be thermodynamically stable to describe another deformation mode. It can be observed that the section of the GR ROS planes on the  $A_{11} = 0$  plane creates the ROS for the MR model (Fig. 4) under the uniaxial deformation mode.

To determine the response functions in Eq. (2) for the GR model, the Cauchy stress tensor obtained using Eq. (83) is compared with the Rivlin-Ericksen representation of stress as given in Eq. (56),

$$s_0 = -p, \quad s_1 = 2[A_{10} + A_{11}(I_2 - 3)], \quad s_2 = -2[A_{01} + A_{11}(I_2 - 3)]$$
 (85)

Using the response functions from Eq. (85) and substituting into Eqs. (5) and (7) to obtain the adscititious inequalities provides

B-E: 
$$A_{10} + \frac{A_{01}}{\lambda} + 3A_{11} \left(\lambda + \frac{1}{\lambda^2} - \frac{1}{\lambda} - 1\right) > 0$$
 (86)

E: 
$$A_{10} + A_{11} \left( 2\lambda + \frac{1}{\lambda^2} - 3 \right) > 0, \quad A_{01} + A_{11} \left( \lambda^2 + \frac{2}{\lambda} - 3 \right) \ge 0$$
 (87)

Note from Eq. (87) that as opposed to the one or two-parameter polynomial models (NH and MR models), the E-inequalities for GR model are dependent on the limiting stretch values (compare Eqs. (58), (66) and (87)). Under the infinitesimal strain assumption ( $\lambda \approx 1$ ), these inequalities converge to those of the MR model as given by Eq. (66), which means that the third model constant can take any real value. The stability region in this situation is the union of first and fifth octant. However, as the material reaches infinite compression or tension,  $A_{11}$  attains a stable lower limit and Eq. (87) finally becomes

$$E_{U-\infty}$$
:  $A_{10} > 0, \quad A_{01} \ge 0, A_{11} > 0$  (88)

To compare B-E inequalities with the T-C inequality given in Eq. (83), a similar approach to the one used in Section 4.2 is used. However, as the ROS for the GR model is a region defined by three-dimensional planes, it is more convenient to compare the components of the unit normal vectors to these planes (instead of slopes), which represent the cosine of angles made by the normal vector with respect to the three axes (in this case  $A_{10}$ ,  $A_{01}$  and  $A_{11}$ ). Following this approach, the normal vector components to the ROS planes corresponding to T-C and B-E inequalities (Eqs. (83) and (86)) are derived as

T-C: 
$$\mathbf{n}^{\text{T-C}} = \left( \left( 1 + \frac{2}{\lambda^3} \right), \left( \frac{3}{\lambda^4} \right), 3 \left( 2\lambda - 1 + \frac{4}{\lambda^5} - \frac{3}{\lambda^4} - \frac{2}{\lambda^3} \right) \right)$$
 (89)

B-E: 
$$\mathbf{n}^{\text{B-E}} = \left\langle 1, \left( \frac{1}{\lambda} \right), 3 \left( \lambda + \frac{1}{\lambda^2} - \frac{1}{\lambda} - 1 \right) \right\rangle \tag{90}$$

where  $\mathbf{n}^{T-C}$  and  $\mathbf{n}^{B-E}$  represent the normal vectors (represented here in the ordered set notation) to the planes defining T-C and B-E inequalities, respectively. Dividing each component of these vectors by its scalar magnitude yields the unit vectors, which are used for further analysis.

Fig. 11 shows the components of unit normal vectors  $\langle \hat{n}_1, \hat{n}_2, \hat{n}_3 \rangle$  for planes defined by T-C and B-E inequalities Eqs. (89) and (90) versus the limiting uniaxial stretch  $\lambda$ . Similar to the MR model, both T-C and B-E inequalities have the same trend with respect to limiting strains in both the compression and tension regimes. Under infinitesimal strains (dotted

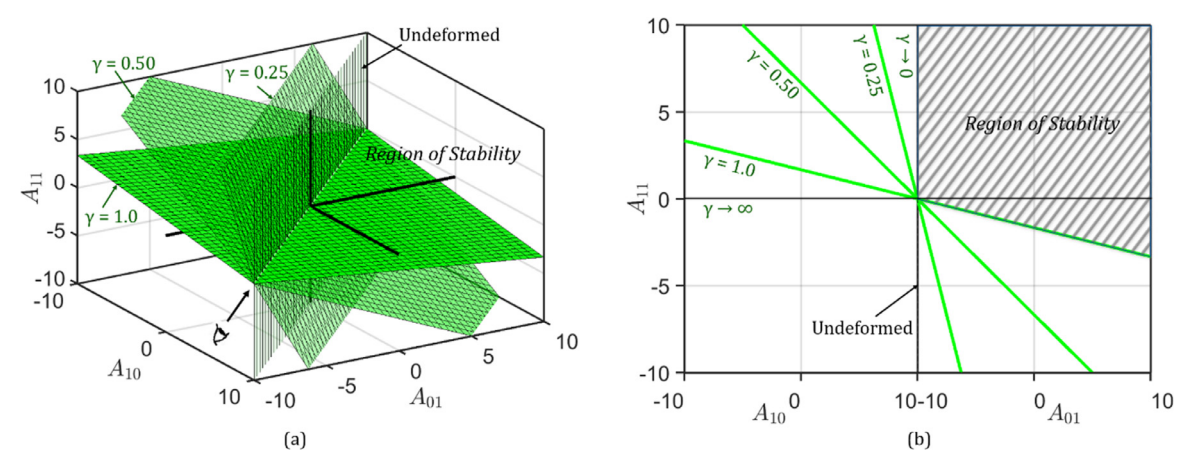


**Fig. 12.** (a) Evolution of the three-dimensional *Region of Stability* for generalized Rivlin model in simple shear deformation mode, with planes representing T-C inequalities plotted for limiting shear strains  $\gamma = 0$ , 0.25, 0.50 and 1.0. (b) Two-dimensional view of the  $A_{10}$ - $A_{01}$ - $A_{11}$  coordinate space as viewed along the line  $A_{10}$ + $A_{01}$ =0 (viewing eye shown in (a)) and hatched *ROS* for  $\gamma = 1.0$  limiting strain.

line  $\lambda=1$ ), the respective unit normal components for both the inequalities are coincident  $(n_i^{\text{T-C}}=n_i^{\text{B-E}},\ i=1,\ 2,\ 3)$ , so that the stability criterion can be defined by the inequality  $A_{10}+A_{01}>0$ . This is also true for extreme limiting stretches  $(\lambda\to 0 \text{ and } \lambda\to\infty)$  when both the inequalities have equal unit normal vectors given as  $\langle 0,0,1\rangle$ . In other words, at extreme limiting strains, the planes representing these two inequalities are parallel to the  $A_{11}=0$  plane, and the stability criterion can be written as a necessary but not sufficient condition given by

$$T-C_{U-\infty}^*, B-E_{U-\infty}^*$$
:  $A_{10}+A_{01}>0, A_{11}>0$  (91)

From Fig. 11, it can be seen that the  $\hat{n}_3$  components (or angles with respect to  $A_{11}$  axis) of the planes defined by these two inequalities have a definite relationship given as  $\hat{n}_3^{\text{T-C}} \geq \hat{n}_3^{\text{B-E}}$  for all possible limiting strains (equality at  $\lambda = 1$ ). This implies that for large finite limiting strains, the T-C inequality poses a more stringent requirement on the lower bound of model constant  $A_{11}$  as compared to the B-E inequality, a difference that is more pronounced in tension than the compression mode as evident from the greater difference between the  $\hat{n}_3$  components of these inequalities in tension. However, as the  $\hat{n}_1$  components (or angles with respect to  $A_{10}$  axis) of these planes intersect in both the compression and tension regions, and there is no common intersection line between these planes, there is no general logical implication between T-C and B-E inequalities under finite limiting strains. Thus, for the GR model

$$B-E \Rightarrow T-C, \quad T-C \Rightarrow B-E$$
 (92)

On the other hand, for a hypothetical material that fails at  $\lambda \to 0$  in compression and  $\lambda \to \infty$  in tension, it is clearly concluded that E-inequalities are excessively stringent and imply both B-E and T-C inequalities, but not vice versa,

$$E_{U-\infty} \Rightarrow B-E_{U-\infty}, \quad E_{U-\infty} \Rightarrow T-C_{U-\infty}$$
 (93)

## 4.3.2. Simple shear

In cases where a simple shear test is used to find GR model constants, the generalized T-C inequality in Eq. (37) becomes

$$A_{10} + A_{01} + 6A_{11}\gamma^2 > 0 (94)$$

Fig. 12(a) shows the three-dimensional *ROS* obtained using Eq. (94) at various limiting strains. Under an infinitesimal strain assumption, the *ROS* is defined by the inequality  $A_{10} + A_{01} > 0$ . This feasibility region of model constants is represented by the half-space in front of the "*Undeformed*" plane (toward first octant), where  $A_{11}$  can take any real value, positive or negative. However, as the limiting shear strain increases, the *ROS* hyperplane tilts about the line  $A_{01} + A_{10} = 0$ , causing the feasibility region to become smaller (see Fig. 12(b) for the two-dimensional section view). For a hypothetical material that fails at infinite shear strain, the thermodynamic stability criteria converges to

$$T-C_{SS-\infty}$$
:  $A_{10} + A_{01} > 0$ ,  $A_{11} > 0$  (95)

For simple shear deformation of a GR material, it is possible to estimate a definite lower bound for the third model constant  $A_{11}$  in terms of the small strain shear modulus using Eq. (94). Mathematically, for a hyperelastic material described using the three-parameter GR model,

T-C: 
$$A_{10} + A_{01} > 0, \ A_{11} \in \left(-\frac{G}{12\gamma_I^2}, \infty\right)$$
 (96)

where G is the initial shear modulus (Eq. (76)), which can be obtained from small strain experiments.

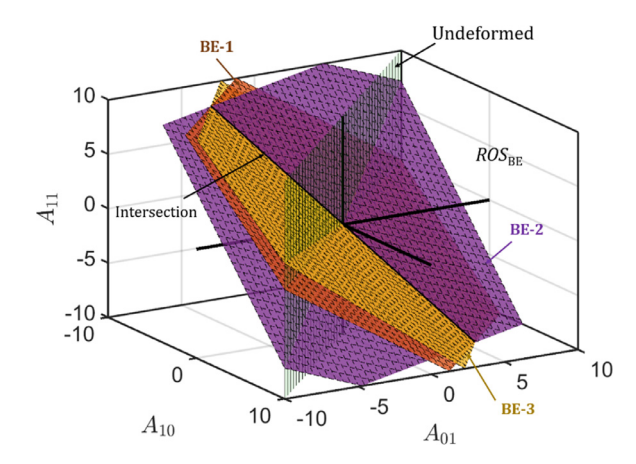


**Fig. 13.** Stability region defined by the Baker-Ericksen inequalities for simple shear deformation ( $\gamma = 0.75$ ).

As an example, Fig. 12(b) shows the ROS for a GR material in simple shear when the limiting shear strain is  $\gamma = 1.0$  (hatched region). Using the response functions from Eq. (85) and the adscititious inequalities,

B-E: 
$$A_{10} + A_{01} + 2A_{11}\gamma^2 > 0$$
,  $A_{10} + A_{11}\gamma^2 + \frac{A_{01} + A_{11}\gamma^2}{\left(1 + \frac{\gamma^2}{2}\right) \pm \frac{\gamma\sqrt{\gamma^2 + 4}}{2}} > 0$  (97)

E: 
$$A_{10} + A_{11}\gamma^2 > 0$$
,  $A_{01} + A_{11}\gamma^2 \ge 0$  (98)

Under infinitesimal limiting strain, E-inequalities take the form in Eq. (66), where  $A_{11}$  can assume any positive or negative real value. However, for materials that fail under a finite value of shear strain, a lower bound can be assigned on the model constant  $A_{11}$  using Eq. (98).

E: 
$$A_{10} > 0$$
,  $A_{01} \ge 0$ ,  $A_{11} \in \left(-\frac{1}{\gamma_{\ell}^2} \min(A_{10}, A_{01}), \infty\right)$  (99)

Note that the lower limit for  $A_{11}$  has a similar form in both T-C and E-inequalities. For a hypothetical material that fails at infinite strain, the form of E-inequalities is given in Eq. (88) (identical to the uniaxial case). E-inequalities for such a material always imply the T-C inequalities, but not vice versa. At an arbitrary limiting shear strain, however, there is no definitive logical relation between the two inequalities.

Unlike the T-C and E-inequalities, B-E inequalities define a set of hyperplanes that do not always pass through the line  $A_{01} + A_{10} = 0$  (nor do they always tilt about this line during evolution with limiting strain). Fig. 13 shows the hyperplanes defined by the B-E inequalities (Eq. (97)) for a nominal limiting shear strain  $\gamma = 0.75$ , where the planes marked as BE-1, BE-2 and BE-3 correspond to the first, second and third equation in Eq. (97), respectively. Note that the three planes intersect at a common line, which can be verified by taking the dot product between the normal vector to BE-1, with the vector along the intersection between planes BE-2 and BE-3 at any arbitrary limiting strain

$$\left\langle \left\langle 1, \frac{1}{\left(1 + \frac{\gamma^2}{2}\right) + \frac{\gamma\sqrt{\gamma^2 + 4}}{2}}, \gamma^2 \left(1 + \frac{1}{\left(1 + \frac{\gamma^2}{2}\right) \pm \frac{\gamma\sqrt{\gamma^2 + 4}}{2}}\right) \right\rangle \times \left\langle 1, \frac{1}{\left(1 + \frac{\gamma^2}{2}\right) + \frac{\gamma\sqrt{\gamma^2 + 4}}{2}}, \gamma^2 \left(1 + \frac{1}{\left(1 + \frac{\gamma^2}{2}\right) \pm \frac{\gamma\sqrt{\gamma^2 + 4}}{2}}\right) \right\rangle \right\rangle \cdot \left\langle 1, 1, 2\gamma^2 \right\rangle = 0, \ \forall \{\gamma \mid \gamma \in \mathbb{R} \land \gamma > 0\}$$

$$(100)$$

where symbols  $\times$  and  $\cdot$  represent vector cross and dot products, respectively. Eq. (100) suggests that the last two B-E inequalities define a stable region that is always a subset of the one defined by the first B-E inequality. Thus, the B-E inequalities in this case reduce to a set of two inequalities as

B-E: 
$$A_{10} + A_{11}\gamma^2 + \frac{A_{01} + A_{11}\gamma^2}{\left(1 + \frac{\gamma^2}{2}\right) \pm \frac{\gamma\sqrt{\gamma^2 + 4}}{2}} > 0$$
 (101)

For infinite limiting shear strains, Eq. (101) takes the form of a necessary but not sufficient stability condition given by

$$B - E_{SS-\infty}^*$$
:  $A_{10} + A_{01} > 0, A_{11} > 0$  (102)

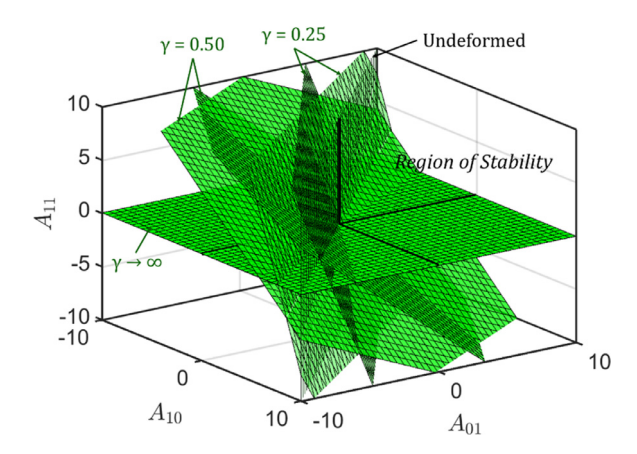


Fig. 14. Region of Stability (3-D) for generalized Rivlin model under pure shear.

From Eqs. (94) and (101), it is concluded that there is no definitive logical relation between the T-C and B-E stability conditions in the simple shear deformation of a GR material, that is, Eq. (92) holds true for this case as well. Furthermore, similar to the uniaxial case, the E-inequalities imply both T-C and B-E inequalities under extreme limiting strain ( $\gamma \to \infty$ ),

$$E_{SS-\infty} \Rightarrow B-E_{SS-\infty}, E_{SS-\infty} \Rightarrow T-C_{SS-\infty}$$
 (103)

#### 4.3.3. Pure shear

Using the ROS coefficients from Table 1, the condition for thermodynamic stability of a GR material in pure shear is defined as

$$A_{10}\left(\frac{1+4\gamma^{2}}{1+\gamma^{2}}\right) + A_{01}\frac{\left(8\gamma^{6} + 18\gamma^{4} + 12\gamma^{2} + 1\right)}{\left(1+\gamma^{2}\right)^{3}} + A_{11}\frac{\gamma^{2}\left(24\gamma^{6} + 56\gamma^{4} + 39\gamma^{2} + 6\right)}{\left(1+\gamma^{2}\right)^{3}} > 0,$$

$$A_{10}\frac{\left(6\gamma^{6} + 14\gamma^{4} + 11\gamma^{2} + 1\right)}{\left(1+\gamma^{2}\right)^{3}} + A_{01}\left(\frac{1+3\gamma^{2}}{1+\gamma^{2}}\right) + A_{11}\frac{\gamma^{2}\left(20\gamma^{6} + 49\gamma^{4} + 37\gamma^{2} + 6\right)}{\left(1+\gamma^{2}\right)^{3}} > 0$$

$$(104)$$

Fig. 14 shows the evolution of ROS in pure shear with limiting shear strain, where the ROS at any particular limiting strain is obtained by taking the intersection of the two inequalities in Eq. (104). Similar to the uniaxial and simple shear cases, under small strain condition, the ROS in the case of pure shear can be defined by the expression  $A_{01} + A_{10} > 0$  where model constant  $A_{11}$  is unrestricted in the real domain. However, unlike the simple shear case, the hyperplanes defining the ROS neither always pass through nor tilt about the line  $A_{01} + A_{10} = 0$  as the limiting strain increases. It is thus not possible to define a stable lower limit for  $A_{11}$  in the form as given in Eq. (96) or (99). Furthermore, the general condition in Eq. (104) can be simplified with a necessary but not sufficient condition when limiting shear strain tends to infinity,

$$T-C_{PS-\infty}^*$$
:  $A_{10} + A_{01} > 0$ ,  $A_{11} > 0$  (105)

The adscititious inequalities in this case can be written as

B-E: 
$$A_{10} + \frac{A_{01}}{\left(1 + \gamma^{2}\right)} + A_{11} \frac{\gamma^{2} \left(\gamma^{4} + 4\gamma^{2} + 2\right)}{\left(1 + \gamma^{2}\right)^{2}} > 0,$$

$$A_{10} + \frac{A_{01}}{\left(1 \mp \frac{\gamma}{\sqrt{\gamma^{2} + 1}}\right)} + A_{11} \gamma^{2} \left(1 + \frac{1 + 2\gamma^{2}}{\left(1 + \gamma^{2} \mp \gamma \sqrt{\gamma^{2} + 1}\right)}\right) > 0$$

$$(106)$$

E: 
$$A_{10} + A_{11}\gamma^2 > 0$$
,  $A_{01} + A_{11}\frac{\gamma^2(1+2\gamma^2)}{1+\gamma^2} \ge 0$  (107)

Under the small strain assumption, B-E and E-inequalities take the forms given in Eqs. (69) and (66), respectively. However, as the limiting strain increases in magnitude, the stability regions dictated by individual adscititious inequalities become smaller. For a hypothetical material that fails at infinite strain, the B-E and E-inequalities take the form given in Eqs. (102) and (88), respectively. Out of these two extreme stability conditions, Eq. (102) is a necessary but not sufficient condition for stability of GR model constants.

Unlike the simple shear case, the three B-E inequalities in pure shear do not intersect at a common plane. Furthermore, none of the three inequalities is redundant or can be merged into the other two for finite limiting shear strain, and the

intersection of individual half-spaces must be taken to visualize the stability region of model constants. Therefore, there is no definite logical relation between B-E and T-C inequalities (Eq. (92)). But, for the limiting case when  $\gamma \to \infty$ ,

$$E_{PS-\infty} \Rightarrow B-E_{PS-\infty}, E_{PS-\infty} \Rightarrow T-C_{PS-\infty}$$
 (108)

For a completely stable GR model, the combined compression, tension and shear data must be used when obtaining material parameters. Even if one out of the three primary deformation mode tests is not considered while fitting the GR model, there is a finite probability that the material parameters will be thermodynamically unstable for that mode.

#### 5. Thermodynamic stability criteria for non-polynomial hyperelastic constitutive models

The polynomial models such as those studied in Section 3 are some of the most commonly used strain-energy density functions in finite element simulations, which accurately capture small to moderately large ranges of strain (Marckmann and Verron, 2006; Tobajas et al., 2016). These type of models, however, have limitations related to the prediction of compressibility and limiting chain extensibility effects (Horgan and Saccomandi, 2003). Many of the novel molecular theory based hyperelastic models are based on complicated functions such as the inverse Langevin function, which is often approximated using Padé approximants (e.g., the Arruda-Boyce model (Arruda and Boyce, 1993), the Perrin model (Gilles, 2000) and the Micro-sphere model (Miehe, 2004)), and connect macro and mesoscopic response of rubber-like materials. In addition, a class of non-polynomial phenomenological models yielded by the modified Rivlin-Signorini method (Horgan and Saccomandi, 2003) are capable of capturing compressibility, limiting-chain extensibility and thermoelastic behavior, and thus are better at qualitatively capturing the mechanical behavior of rubbers than polynomial models. Although these models are more complicated and are generally not available in commercial finite element programs, they are promising in that they aim to capture some typical material behaviors that cannot be modeled by classical polynomial models (e.g., Mullins, Payne and limiting extensibility effects).

Thus, in this section, the applicability of the thermodynamics-based approach for finding constitutive inequalities for non-polynomial hyperelastic models is demonstrated. Note, it is not possible to derive generalized inequalities for these functions, which do not have a general form such as Eqs. (20) and (21) for the polynomial models. Furthermore, unlike the polynomial models where flat hyperplanes define the ROS in a particular deformation mode, the ROS for non-polynomial models (e.g., exponential/logarithmic functions) are defined by hypersurfaces, which makes their analysis a non-trivial task. For brevity, constitutive inequalities for only one model, the Fung-Demiray model (Demiray, 1972; Fung, 1967) are derived, which is a simple two-parameter exponential form that has been used in modeling biological materials such as porcine brain (Rashid et al., 2013, 2014), spleen (Davies et al., 2002), and liver tissues (Chui et al., 2004) in a variety of primary deformation modes. A similar procedure can be adopted to define bounds on model constants of other non-polynomial model types.

#### 5.1. Fung-Demiray model

The Fung-Demiray (FD) model has a strain energy density function W given by

$$W = \frac{C_1}{2C_2} \left( e^{C_2(I_1 - 3)} - 1 \right) \tag{109}$$

where model constants  $C_1$  and  $C_2$  represent the initial shear modulus and stiffening parameter, respectively.

# 5.1.1. Uniaxial deformation (compression or tension)

Using the first principal invariant  $I_1$  (Eq. (28)) and the general thermodynamic stability criterion for uniaxial deformation (Eq. (29)),

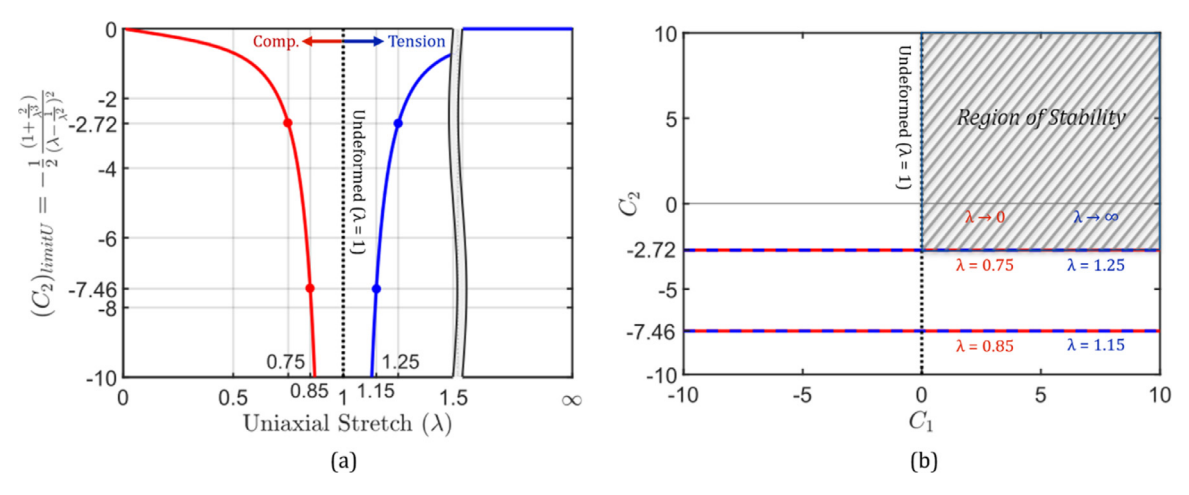
$$\frac{d\phi_U(\lambda)}{d\lambda} = C_1 \left(\lambda - \frac{1}{\lambda^2}\right) e^{C_2 \left(\lambda^2 + \frac{2}{\lambda} - 3\right)} - T_{11} = 0 \tag{110}$$

$$\frac{d^2 \phi_U(\lambda)}{d\lambda^2} = C_1 e^{C_2 \left(\lambda^2 + \frac{2}{\lambda} - 3\right)} \left( 1 + \frac{2}{\lambda^3} + 2C_2 \left(\lambda - \frac{1}{\lambda^2}\right)^2 \right) > 0 \tag{111}$$

Eq. (110) yields the nominal tensile stress in the loading direction. Eq. (111), on the other hand, is the T-C inequality that defines the ROS. Note that as the exponent is always positive regardless of the limiting strain, the T-C inequality for the FD constitutive model under uniaxial deformation is

$$C_1\left(1+\frac{2}{\lambda^3}+2C_2\left(\lambda-\frac{1}{\lambda^2}\right)^2\right)>0\tag{112}$$

Unlike the T-C inequalities for polynomial models that are linear with respect to model constants, the ROS for exponential/logarithmic models are defined by nonlinear hypersurfaces. Under the infinitesimal strain condition ( $\lambda \approx 1$ ), the coefficient  $C_2$  in Eq. (112) vanishes and the stability criterion reduces to  $C_1 > 0$  (no bound on  $C_2$ ). However, for arbitrary



limiting strain values,  $C_2$  has a finite lower bound,  $(C_2)_{limitU}$ , which is a function of the limiting uniaxial stretch  $\lambda_L$ . The T-C inequalities can thus be defined as

T-C: 
$$C_1 > 0, \quad C_2 \in \left( \left( (C_2)_{limitU} = -\frac{1}{2} \frac{\left(1 + \frac{2}{\lambda_L^3}\right)}{\left(\lambda_L - \frac{1}{\lambda_L^2}\right)^2} \right), \infty \right)$$
 (113)

Fig. 15(a) shows the evolution of the lower bound  $(C_2)_{limitU}$  with limiting material strain (or stretch). In this figure, the neighborhood of the line  $\lambda=1$  represents the small strain condition, at which  $(C_2)_{limitU}$  is negative infinity (i.e., no bound on  $C_2$ ). This is also reflected in the ROS (Fig. 15(b)), which covers the entire first and fourth quadrant under such conditions. As the limiting strain reaches extreme values  $(\lambda_L \to 0 \text{ and/or } \lambda_L \to \infty)$ ,  $(C_2)_{limitU}$  becomes zero, and the ROS reduces to the first quadrant  $(C_1 > 0, C_2 > 0)$ . For finite values of stretch, the ROS extends into the fourth quandrant as shown in Fig.15b, rendering the values of  $C_2$  to be negative (e.g., hatched portion in Fig. 15(b) for  $\lambda=0.75$  in compression or  $\lambda=1.25$  in tension).

# 5.1.2. Simple shear

For simple shear deformation, the thermodynamic stability criterion (Eq. (34)) can be derived using principal invariants of C from Eq. (35) as

$$\frac{d\phi_{SS}(\gamma)}{d\gamma} = C_1 \gamma e^{C_2 \gamma^2} - T_{21} = 0 \tag{114}$$

$$\frac{d^2\phi_{SS}(\gamma)}{d\gamma^2} = C_1 e^{C_2 \gamma^2} \left( 1 + 2C_2 \gamma^2 \right) > 0 \tag{115}$$

While Eq. (114) yields the nominal shear stress  $T_{21}$ , Eq. (115) defines the ROS in simple shear for the FD model. Similar to the uniaxial deformation mode, the ROS in simple shear under infinitesimal limiting strain becomes  $C_1 > 0$  (unbounded  $C_2$ ). However, for a finite limiting shear strain  $\gamma$ ,  $C_2$  has a defined lower limit. In general, the thermodynamic stability criterion for the FD model in simple shear deformation is given as

T-C: 
$$C_1 > 0, \quad C_2 \in \left(\left((C_2)_{limitSS} = -\frac{1}{2\gamma_L^2}\right), \infty\right)$$
 (116)

where  $\gamma_L$  is the limiting shear strain.

Fig. 16(a) shows the variation of lower bound of  $C_2$  for simple shear  $((C_2)_{limitSS})$  and pure shear  $((C_2)_{limitPS})$  modes as a function of the limiting shear strain. As shown in the figure,  $(C_2)_{limitSS}$  evolves from being negative infinity under small strain condition  $(\gamma \approx 0)$ , to zero under extreme limiting shear strains  $(\gamma \to \infty)$ . Correspondingly, the ROS (Fig. 16(b)) shrinks from an initial region covering the entire first and fourth quadrants  $(C_1 > 0)$ , unbounded  $(C_2)$ , to only the first quadrant  $(C_1 > 0)$ ,  $(C_2 > 0)$ . It is evident that similar to the uniaxial case, the value of model constant  $(C_2)$  can be negative and follows the inequality given in Eq. (116).

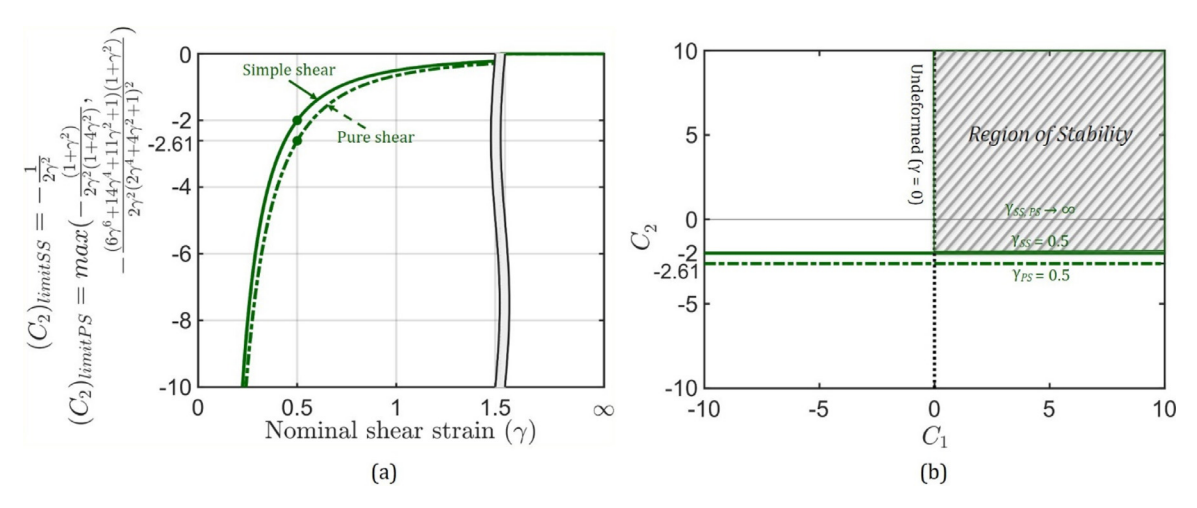


**Fig. 16.** (a) Lower bound of  $C_2$  as a function of limiting shear strain, and (b) the resulting evolution of the *Region of Stability* for the Fung-Demiray model in simple and pure shear deformation modes. Hatched region in (b) represents the *ROS* at limiting strain  $\gamma = 0.5$  in simple shear, which is obtained by taking the intersection of small strain *ROS*,  $C_1 > 0$ , and  $C_2 > -2$  (( $C_2$ )<sub>limitSS</sub> = -2 at  $\gamma = 0.5$ ).

#### 5.1.3. Pure shear

Using the thermodynamic stability criteria defined in Eq. (49) and the principal invariants of  $\mathbf{C}$  in the case of pure shear from Eq. (49b),

$$\frac{d\phi_{PS}(\gamma)}{d\gamma}\bigg|_{\dot{a}=0} = C_1 \gamma e^{C_2 \gamma^2} - \frac{T_{21}}{\left(1 + \gamma^2\right)^{3/2}} = 0 \tag{117a}$$

$$\frac{d\phi_{PS}(\gamma)}{d\gamma}\bigg|_{\dot{b}=0} = C_1 \gamma \left(\frac{2\gamma^4 + 4\gamma^2 + 1}{\left(1 + \gamma^2\right)^2}\right) e^{C_2 \frac{\gamma^2 \left(1 + 2\gamma^2\right)}{1 + \gamma^2}} - \frac{T_{21}}{1 + \gamma^2} = 0$$
(117b)

$$\frac{d^2\phi_{PS}(\gamma)}{d\gamma^2}\bigg|_{\dot{q}=0} = C_1 e^{C_2\gamma^2} \left(\frac{1+4\gamma^2}{1+\gamma^2} + 2C_2\gamma^2\right) > 0$$
 (118a)

$$\frac{d^{2}\phi_{PS}(\gamma)}{d\gamma^{2}}\bigg|_{\dot{b}=0} = \frac{C_{1}e^{C_{2}\frac{\gamma^{2}\left(1+2\gamma^{2}\right)}{1+\gamma^{2}}}}{\left(1+\gamma^{2}\right)^{3}}\left(\left(6\gamma^{6}+14\gamma^{4}+11\gamma^{2}+1\right)+\frac{2C_{2}\gamma^{2}\left(2\gamma^{4}+4\gamma^{2}+1\right)^{2}}{1+\gamma^{2}}\right) > 0 \tag{118b}$$

From Eqs. (117a) and (117b), the nominal shear stresses as a funciton of shear strain can be obtained. The second stability criterion (intersection of inequalities in Eqs. (118a) and (118b)) define the ROS, which is nonlinear similar to all previous cases for the FD model. For any arbitrary limiting shear strain  $\gamma_L$ , the first model constant follows the inequality  $C_1 > 0$ . However, the model constant  $C_2$  is bounded on the lower end, so that the general T-C inequality in pure shear becomes

T-C: 
$$C_1 > 0$$
,  $C_2 \in \left( \left( (C_2)_{limitPS} = \max \left( -\frac{\left(1 + \gamma_L^2\right)}{2\gamma_L^2 \left(1 + 4\gamma_L^2\right)}, -\frac{\left(6\gamma_L^6 + 14\gamma_L^4 + 11\gamma_L^2 + 1\right)\left(1 + \gamma_L^2\right)}{2\gamma_L^2 \left(2\gamma_L^4 + 4\gamma_L^2 + 1\right)^2} \right) \right), \infty \right)$  (119)

As shown in Fig. 16(a), similar to the uniaxial and simple shear deformations, the ROS in pure shear evolves from a region defined by  $C_1 > 0$  (unbounded  $C_2$ ) in small strain condition, to the one defined by the inequality  $C_1 > 0$ ,  $C_2 > 0$  under extreme limiting shear strains ( $(C_2)_{limitPS}$  tends to zero as  $\gamma \to \infty$ ).

Many recent publications (e.g., Destrade et al., 2014; Goriely, 2017; Horgan, 2015; Jiang et al., 2015; Wex et al., 2015) have incorrectly stated that the model constants of the FD model must be positive, without any rigorous stability analysis. In this work, it is demonstrated from first principles that the bounds on the FD model constants evolve as a function of the limiting material strain, and are unconditionally positive only under the infinite limiting strain condition. For hyperelastic materials under small to moderate limiting strains, this stringent requirement can be relaxed so that  $C_2$  can assume negative values.

#### 6. Summary and conclusions

A tensorial form of a thermodynamic stability criterion is derived for an isotropic hyperelastic solid undergoing isothermal deformation. This formulation requires that a given state of deformation is stable if the available energy attains its minimum at that state. Using this criterion, a generalized thermodynamic constitutive inequality (T-C inequality) of the form  $\sum_{m+n=1}^{\infty} A_{mn} \zeta_{mn}(\varepsilon) > 0$  is defined for the polynomial form of hyperelastic constitutive models, which is a function of both

the deformation mode and limiting strain. Individual T-C inequalities are formulated for compression, tension and shear deformation modes, which are required in the numerical estimation of model constants for incompressible hyperelastic solids.

For the NH model, which is the simplest hyperelastic model, a single constitutive inequality  $A_{10} > 0$  is derived, which is invariant to the considered deformation mode, limiting strain value and the inequality type (T-C, B-E or E). The model constant obtained from any of the primary deformation experiments, is thus thermodynamically stable to yield a physically reasonable response in another deformation mode, or for a complex three-dimensional stress state. However, it is noted that this propensity for a thermodynamically stable response does not guarantee model accuracy, and experiments simulating multiple deformation modes are recommended, whenever possible.

For the two and three-parameter polynomial hyperelastic models, the T-C inequalities differ from one deformation mode to another. However, in each of the three primary deformation modes, the ROS for model constants evolves in a similar fashion with limiting strain, being largest for small strain elasticity, and finally converging to a smaller region at infinite limiting strains. For the two-parameter MR material, the largest (necessary condition for stability) and the smallest (sufficient condition for stability) ROS are defined by inequalities  $A_{10} + A_{01} > 0$  and  $A_{10} > 0$ ,  $A_{01} > 0$ , respectively. This observation leads to a possible explanation that the ability of rubber-like materials to undergo very large deformations is the reason behind the success of E-inequalities (defined as  $A_{10} > 0$ ,  $A_{01} > 0$  for the MR model) for these materials. For example, early experiments by Treloar (1944) on vulcanized natural rubber registered deformations of 750% in tension, 500% in pure shear, and 450% in equibiaxial tension. For decades, data from such large strain experiments have been used to develop strain energy functions and assess constitutive inequalities. Clearly, under such extreme strains, the model constants followed the converged T-C inequality, which is equivalent to the general E-inequality. However, the term hyperelastic is no longer synonymous to rubber, and a number of novel materials ranging from additively manufactured photopolymers (Liljenhjerte et al., 2016) to biological tissues and hydrogels (Avril, 2017; Rashid et al., 2013; Shearer, 2015) are successfully modeled using hyperelastic constitutive models. These materials remain hyperelastic under small to moderate strains, and thus the excessively stringent E-inequalities are not expected to correctly limit the model constants or the forms of the strain energy density function defining their mechanical behavior. As a common observation, E-inequalities imply both B-E and T-C inequalities, but these two inequalities do not show a logical relationship among themselves. Nevertheless, the trend of parameter restrictions with limiting strain is similar in both B-E and T-C inequalities, making the former more accurate for small to moderate strain elastic materials than E-inequalities.

In case of the three-parameter GR model, the ROS shrinks from the region defined by  $A_{10} + A_{01} > 0$  at small limiting strains to a necessary and sufficient condition given as  $A_{01} > 0$ ,  $A_{10} > 0$ , and  $A_{11} > 0$  for materials (hypothetically) that are hyperelastic until infinite limiting strains. The latter extreme condition ROS is essentially the first octant in the  $A_{10}$ - $A_{01}$ - $A_{11}$  coordinate space, and coincides with the E-inequalities under such conditions. The common trend of a shrinking ROS in polynomial hyperelastic models with increasing limiting strain values across various deformation modes is also visible in the exponential FD model. Here, the lower limit of the model constant  $C_2$  varies from negative infinity (unbounded) under small limiting strains to zero in extreme conditions, while the model constant  $C_1$ , being the initial shear modulus is required to be positive. Regardless of the model type, it appears that E-inequalities are always the most conservative constitutive inequalities.

Importantly, it is demonstrated that the model constants obtained using one experiment might not yield a naturally plausible response for a different type of deformation (primary or three-dimensional). This observation is especially striking in the case of the two and three-parameter polynomial models where compression and tension deformations impose opposing restrictions on the model constants (see Figs. 5(a), 5(b) and 10). It is important, thus, to consider both of these modes in the determination of material parameters. Furthermore, the necessary and sufficient condition for stability in shear mode for an MR material is a function of the initial shear modulus (Eq. (75)), which can be determined via small strain experiments or from Eq. (76) using model constants obtained by uniaxial tests. While this property may help reduce dependency on shear data (if  $A_{10}$ ,  $A_{01} \in (-G/2, G)$ ) for this model, no such simplification is possible in case of the GR model where T-C inequalities yield ROS that are complicated three-dimensional spaces. Similar conclusion can be drawn for the FD model in which lower bounds on parameter  $C_2$  for the three primary deformation modes are functions of their respective limiting strains.

Finally, the proposed mathematical framework can be used as a filter to reject unfeasible model constants potentially resulting from flawed experiments and/or numerical procedures, by plotting them in that particular deformation mode's ROS plot and verifying if they fall in the stable region. In addition, if the limiting strain values in all the homogeneous deformation modes are known (or can be estimated), then conclusions can be drawn about whether the model constants obtained from one type of experiment (e.g., tension) will yield a thermodynamically stable response in another deformation mode (say compression).

# Acknowledgements

This work was supported by the National Science Foundation under Grant No. CMMI-1634188. The authors are grateful to the reviewers whose comments improved the quality of this work.

# References

Avril, S., 2017. Material Parameter Identification and Inverse Problems in Soft Tissue Biomechanics, CISM International Centre for Mechanical Sciences. Springer International Publishing, Cham. https://doi.org/10.1007/978-3-319-45071-1.

Baker, M., Ericksen, J.L., 1954. Inequalities restricting the form of the stress-deformation relations for isotropic elastic solids and Reiner-Rivlin fluids. J. Washingt. Acad. Sci. 44, 33–35.

Ball, J.M., James, R.D., 2002. The scientific life and influence of Clifford Ambrose Truesdell III. Arch. Ration. Mech. Anal 161, 1–26. https://doi.org/10.1007/s002050100178.

Beatty, M.F., 2008. On constitutive models for limited elastic, molecular based materials. Math. Mech. Solids 13, 375–387. https://doi.org/10.1177/

Beatty, M.F., 2003. An average-stretch full-network model for rubber elasticity. J. Elast. 70, 65-86. https://doi.org/10.1023/B:ELAS.0000005553.38563.91.

Beda, T., 2014. An approach for hyperelastic model-building and parameters estimation a review of constitutive models. Eur. Polym. J. 50, 97–108. https://doi.org/10.1016/j.eurpolymj.2013.10.006.

Berselli, G., Vertechy, R., Pellicciari, M., Vassur, G., 2011. Hyperelastic modeling of rubber-like photopolymers for additive manufacturing processes. In:
Pellicciari, M., Hoque, M.E. (Eds.), Rapid Prototyping Technology - Principles and Functional Requirements. InTech, Rijeka Ch. 6 https://doi.org/10.5772/20174

Carroll, M.M., 2011. A strain energy function for vulcanized rubbers. J. Elast. 103, 173-187. https://doi.org/10.1007/s10659-010-9279-0.

Casaroli, G., Galbusera, F., Jonas, R., Schlager, B., Wilke, H.-J., Villa, T., 2017. A novel finite element model of the ovine lumbar intervertebral disc with anisotropic hyperelastic material properties. PLoS One 12, e0177088. https://doi.org/10.1371/journal.pone.0177088.

Chui, C., Kobayashi, E., Chen, X., Hisada, T., Sakuma, I., 2004. Combined compression and elongation experiments and non-linear modelling of liver tissue for surgical simulation. Med. Biol. Eng. Comput. 42, 787–798. https://doi.org/10.1007/BF02345212.

Coleman, B.D., Noll, W., 1959. On the thermostatics of continuous media. Arch. Ration. Mech. Anal. 4, 97-128. https://doi.org/10.1007/BF00281381.

Czerner, M., Fellay, L.S., Suárez, M.P., Frontini, P.M., Fasce, L.A., 2015. Determination of elastic modulus of gelatin gels by indentation experiments. Procedia Mater. Sci. 8, 287–296. https://doi.org/10.1016/j.mspro.2015.04.075.

Davies, P.J., Carter, F.J., Cuschieri, A., 2002. Mathematical modelling for keyhole surgery simulations: a biomechanical model for spleen tissue. IMA J. Appl. Math. 67, 41–67. https://doi.org/10.1093/imamat/67.1.41.

Demiray, H., 1972. A note on the elasticity of soft biological tissues. J. Biomech. 5, 309-311. https://doi.org/10.1016/0021-9290(72)90047-4.

Destrade, M., Gilchrist, M.D., Murphy, J.G., 2010. Onset of nonlinearity in the elastic bending of blocks. J. Appl. Mech. 77, 061015. https://doi.org/10.1115/1. 4001282.

Destrade, M., Horgan, C.O., Murphy, J.G., 2015. Dominant negative Poynting effect in simple shearing of soft tissues. J. Eng. Math. 95, 87–98. https://doi.org/10.1007/s10665-014-9706-5.

Destrade, M., Murphy, J.G., Saccomandi, G., 2012. Simple shear is not so simple. Int. J. Non. Linear. Mech. 47, 210–214. https://doi.org/10.1016/j.ijnonlinmec. 2011.05.008.

Destrade, M., Ogden, R.W., Sgura, I., Vergori, L., 2014. Straightening: existence, uniqueness and stability. Proc. R. Soc. A Math. Phys. Eng. Sci. 470. 20130709–20130709 https://doi.org/10.1098/rspa.2013.0709.

Destrade, M., Saccomandi, G., Sgura, I., 2017. Methodical fitting for mathematical models of rubber-like materials. Proc. R. Soc. A Math. Phys. Eng. Sci. 473, 20160811. https://doi.org/10.1098/rspa.2016.0811.

Fung, Y., 1967. Elasticity of soft tissues in simple elongation. Am. J. Physiol. Content 213, 1532–1544. https://doi.org/10.1152/ajplegacy.1967.213.6.1532.

Gent, A.N., 1996. A new constitutive relation for rubber. Rubber Chem. Technol. 69, 59-61. https://doi.org/10.5254/1.3538357.

Gilles, P., 2000. Analytic stress-strain relationship for isotropic network model of rubber elasticity. Comptes Rendus l'Académie des Sci. - Ser. IIB - Mech. 328, 5–10. https://doi.org/10.1016/S1287-4620(00)88409-4.

Goriely, A., 2017. The Mathematics and Mechanics of Biological Growth, Interdisciplinary Applied Mathematics. Springer New York, New York, NY https://doi.org/10.1007/978-0-387-87710-5.

Hamilton, M.F., Ilinskii, Y.A., Zabolotskaya, E.A., 2004. Separation of compressibility and shear deformation in the elastic energy density (L). J. Acoust. Soc. Am. 116, 41–44. https://doi.org/10.1121/1.1736652.

Haupt, P., 2002. Continuum Mechanics and Theory of Materials, Advanced Texts in Physics. Springer Berlin Heidelberg, Berlin, Heidelberg https://doi.org/10. 1007/978-3-662-04775-0

Hill, R., 1968. On constitutive inequalities for simple materials-I. J. Mech. Phys. Solids 16, 229-242. https://doi.org/10.1016/0022-5096(68)90031-8.

Hin, R., 1500. On Constitute inequalities for simple materials—i. J. Meeti. Figs. 3501ds 10, 223–242. https://doi.org/10.1016/j.iinonlinmec.2014.05.010.

Horgan, C.O., Murphy, J.G., 2015. Reverse Poynting effects in the torsion of soft biomaterials. J. Elast. 118, 127–140. https://doi.org/10.1007/s10659-014-9482-5.

Horgan, C.O., Saccomandi, G., 2003. Finite thermoelasticity with limiting chain extensibility. J. Mech. Phys. Solids 51, 1127–1146. https://doi.org/10.1016/ S0022-5096(02)00144-8.

Janmey, P.A., McCormick, M.E., Rammensee, S., Leight, J.L., Georges, P.C., MacKintosh, F.C., 2007. Negative normal stress in semiflexible biopolymer gels. Nat. Mater. 6, 48–51. https://doi.org/10.1038/nmat1810.

Jiang, Y., Li, G., Qian, L-X., Liang, S., Destrade, M., Cao, Y., 2015. Measuring the linear and nonlinear elastic properties of brain tissue with shear waves and inverse analysis. Biomech. Model. Mechanobiol. 14. 1119–1128. https://doi.org/10.1007/s10237-015-0658-0.

Kim, N.-H., 2015. Introduction to Nonlinear Finite Element Analysis. Springer US, New York, NY https://doi.org/10.1007/978-1-4419-1746-1.

Kroon, M., 2011. An 8-chain model for rubber-like materials accounting for non-affine chain deformations and topological constraints. J. Elast. 102, 99–116. https://doi.org/10.1007/s10659-010-9264-7.

Kumar, N., Rao, V.V., 2016. Hyperelastic Mooney-Rivlin model: determination and physical interpretation of material constants. MIT Int. J. Mech. Eng. 6, 43-46.

Leclerc, G.E., Debernard, L., Foucart, F., Robert, L., Pelletier, K.M., Charleux, F., Ehman, R., Ho Ba Tho, M.-C, Bensamoun, S.F, 2012. Characterization of a hyper-viscoelastic phantom mimicking biological soft tissue using an abdominal pneumatic driver with magnetic resonance elastography (MRE). J. Biomech. 45, 952–957. https://doi.org/10.1016/ji.jbiomech.2012.01.017.

Lee, E.H., 1973. Some restrictions on constitutive equations; discussion paper. In: Domingos, J.J.D., Nina, M.N.R., Whitelaw, J.H. (Eds.), Foundations of Continuum Thermodynamics. Macmillan Education UK, London, pp. 251–258. https://doi.org/10.1007/978-1-349-02235-9\_13.

Liljenhjerte, J., Upadhyaya, P., Kumar, S., 2016. Hyperelastic strain measurements and constitutive parameters identification of 3D printed soft polymers by image processing. Addit. Manuf. 11, 40–48. https://doi.org/10.1016/j.addma.2016.03.005.

Liu, I.-S., 2012. A note on the Mooney-Rivlin material model. Contin. Mech. Thermodyn. 24, 583-590. https://doi.org/10.1007/s00161-011-0197-6.

Malvern, L.E., 1969. Introduction to the mechanics of a continuous medium. Prentice Hall, Englewood Cliffs, USA.

Mansouri, M.R., Darijani, H., 2014. Constitutive modeling of isotropic hyperelastic materials in an exponential framework using a self-contained approach. Int. J. Solids Struct. 51, 4316–4326. https://doi.org/10.1016/j.ijsolstr.2014.08.018.

Marckmann, G., Verron, E., 2006. Comparison of hyperelastic models for rubber-like materials. Rubber Chem. Technol. 79, 835–858. https://doi.org/10.5254/

Marzano, S., 1983. An interpretation of Baker-Ericksen inequalities in uniaxial deformation and stress. Meccanica 18, 233–235. https://doi.org/10.1007/BF02128248.

McLellan, A.G., 1975. The Coleman-Noll inequality in thermodynamics. J. Phys. A. Math. Gen. 8, 1256-1259. https://doi.org/10.1088/0305-4470/8/8/010.

Miehe, C., 2004. A micro-macro approach to rubber-like materials?Part I: the non-affine micro-sphere model of rubber elasticity. J. Mech. Phys. Solids 52, 2617–2660. https://doi.org/10.1016/j.jmps.2004.03.011.

Mihai, L.A., Budday, S., Holzapfel, G.A., Kuhl, E., Goriely, A., 2017. A family of hyperelastic models for human brain tissue. J. Mech. Phys. Solids 106, 60–79. https://doi.org/10.1016/j.jmps.2017.05.015.

Mihai, L.A., Goriely, A., 2011. Positive or negative Poynting effect? The role of adscititious inequalities in hyperelastic materials. Proc. R. Soc. A Math. Phys. Eng. Sci. 467, 3633–3646. https://doi.org/10.1098/rspa.2011.0281.

Moon, H., Truesdell, C., 1974. Interpretation of adscititious inequalities through the effects pure shear stress produces upon an isotropie elastic solid. Arch. Ration. Mech. Anal. 55, 1–17. https://doi.org/10.1007/BF00282431.

Mooney, M., 1940. A theory of large elastic deformation. J. Appl. Phys. 11, 582-592. https://doi.org/10.1063/1.1712836.

Noll, W., 1958. A mathematical theory of the mechanical behavior of continuous media. Arch. Ration. Mech. Anal. 2, 197–226. https://doi.org/10.1007/

Normand, V., Lootens, D.L., Amici, E., Plucknett, K.P., Aymard, P., 2000. New insight into agarose gel mechanical properties. Biomacromolecules 1, 730–738. https://doi.org/10.1021/bm005583j.

Ogden, R.W., 1972. Large deformation isotropic elasticity: on the correlation of theory and experiment for compressible rubberlike solids. Proc. R. Soc. A Math. Phys. Eng. Sci. 328, 567–583. https://doi.org/10.1098/rspa.1972.0096.

Ogden, R.W., Saccomandi, G., Sgura, I., 2004. Fitting hyperelastic models to experimental data. Comput. Mech 34, 484–502. https://doi.org/10.1007/s00466-004-0593-y.

Pavan, T.Z., Madsen, E.L., Frank, G.R., Adilton, O, Carneiro, A, Hall, T.J, 2010. Nonlinear elastic behavior of phantom materials for elastography. Phys. Med. Biol. 55, 2679–2692. https://doi.org/10.1088/0031-9155/55/9/017.

Pucci, E., Saccomandi, G., 2002. A note on the Gent model for rubber-like materials. Rubber Chem. Technol. 75, 839–852. https://doi.org/10.5254/1.3547687. Puglisi, G., Saccomandi, G., 2016. Multi-scale modelling of rubber-like materials and soft tissues: an appraisal. Proc. R. Soc. A Math. Phys. Eng. Sci. 472, 20160060. https://doi.org/10.1098/rspa.2016.0060.

Rashid, B., Destrade, M., Gilchrist, M.D., 2014. Mechanical characterization of brain tissue in tension at dynamic strain rates. J. Mech. Behav. Biomed. Mater. 33, 43–54. https://doi.org/10.1016/j.jmbbm.2012.07.015.

Rashid, B., Destrade, M., Gilchrist, M.D., 2013. Mechanical characterization of brain tissue in simple shear at dynamic strain rates. J. Mech. Behav. Biomed. Mater. 28, 71–85. https://doi.org/10.1016/j.jmbbm.2013.07.017.

Rivlin, R.S., 1997. Some topics in finite elasticity. In: Barenblatt, G.I, Joseph, D.D. (Eds.), Collected Papers of R.S. Rivlin. Springer New York, New York, NY, pp. 360–389. https://doi.org/10.1007/978-1-4612-2416-7\_25.

Rivlin, R.S., 1973. Some Restrictions on Constitutive Equations, in: Foundations of Continuum Thermodynamics. Macmillan Education UK, London, pp. 229–249. https://doi.org/10.1007/978-1-349-02235-9\_12.

Rivlin, R.S., 1948a. Large elastic deformations of isotropic materials. I. Fundamental concepts. Philos. Trans. R. Soc. A Math. Phys. Eng. Sci. 240, 459–490. https://doi.org/10.1098/rsta.1948.0002.

Rivlin, R.S., 1948b. Large elastic deformations of isotropic materials. IV. Further Developments of the General Theory. Philos. Trans. R. Soc. A Math. Phys. Eng. Sci. 241, 379–397. https://doi.org/10.1098/rsta.1948.0024.

Rivlin, R.S., 1948c. Large elastic deformations of isotropic materials. II. Some uniqueness theorems for pure, homogeneous deformation. Philos. Trans. R. Soc. A Math. Phys. Eng. Sci. 240, 491–508. https://doi.org/10.1098/rsta.1948.0003.

Saccomandi, G., 2018. Ut vis sic tensio. Theor. Appl. Mech. 45, 1-15. https://doi.org/10.2298/TAM170703011S.

Sasson, A., Patchornik, S., Eliasy, R., Robinson, D., Haj-Ali, R., 2012. Hyperelastic mechanical behavior of chitosan hydrogels for nucleus pulposus replacement—Experimental testing and constitutive modeling. J. Mech. Behav. Biomed. Mater. 8, 143–153. https://doi.org/10.1016/j.jmbbm.2011.12.008. Seth, B.R., 1962. Generalized strain measure with applications to physical problems, in: IUTAM symposium on second order effects in elasticity, plasticity and fluid mechanics. Haifa.

Shearer, T., 2015. A new strain energy function for the hyperelastic modelling of ligaments and tendons based on fascicle microstructure. J. Biomech. 48, 290–297. https://doi.org/10.1016/j.jbiomech.2014.11.031.

Signorini, A., 1955. Trasformazioni termoelastiche finite. Ann. di Mat. Pura ed Appl. Ser. 4 (39), 147-201. https://doi.org/10.1007/BF02410769.

Tang, J., Tung, M.A., Lelievre, J., Zeng, Y., 1997. Stress-strain relationships for gellan gels in tension, compression and torsion. J. Food Eng. 31, 511–529. https://doi.org/10.1016/S0260-8774(96)00087-8.

Tobajas, R., Ibartz, E., Gracia, L., 2016. A comparative study of hyperelastic constitutive models to characterize the behavior of a polymer used in automotive engines. In: Proceedings of 2nd International Electronic Conference on Materials. MDPI, Basel, Switzerland, p. A002. https://doi.org/10.3390/ecm-2-A002.

Treloar, L.R.G., 1975. The physics of rubber elasticity, monographs on the physics and chemistry of materials. Oxford University Press, USA. Treloar, L.R.G., 1944a. The elasticity of a network of long-chain molecules. II. Rubber Chem. Technol. 17, 296–302. https://doi.org/10.5254/1.3546653.

Treloar, L.R.G., 1944b. Stress-strain data for vulcanised rubber under various types of deformation. Trans. Faraday Soc. 40, 59. https://doi.org/10.1039/tf9444000059.

Treloar, L.R.G., 1943. The elasticity of a network of long-chain molecules. I. Rubber Chem. Technol. 16, 746-751. https://doi.org/10.5254/1.3540158.

Trinh, T.Q., Sorber, J., Gerlach, G., 2009. Design, simulation and experimental characteristics of hydrogel-based piezoresistive pH sensors. In: Physics and Engineering of New Materials. Springer Berlin Heidelberg, Berlin, Heidelberg, pp. 287–294. https://doi.org/10.1007/978-3-540-88201-5\_33.

Truesdell, C., 1956. Das ungelöste Hauptproblem der endlichen Elastizitätstheorie. ZAMM - Zeitschrift für Angew. Math. und Mech. 36, 97–103. https://doi.org/10.1002/zamm.19560360304.

Truesdell, C., 1952. The mechanical foundations of elasticity and fluid dynamics. I. Ration, Mech. Anal. 1, 125–300.

Truesdell, C., Toupin, R., 1963. Static grounds for inequalities in finite strain of elastic materials. Arch. Ration. Mech. Anal. 12, 1–33. https://doi.org/10.1007/BF00281217.

Wex, C., Arndt, S., Stoll, A., Bruns, C., Kupriyanova, Y., 2015. Isotropic incompressible hyperelastic models for modelling the mechanical behaviour of biological tissues: a review. Biomed. Eng. / Biomed. Tech. 60, 577–592. https://doi.org/10.1515/bmt-2014-0146.



**Kshitiz Upadhyay** is a doctoral student at the Laboratory for Dynamic Response of Advanced Materials (LDRAM) at the University of Florida. His research focuses on the experimental and analytical modeling of the mechanical behavior of polymeric gels. Prior to his graduate study, he was a Mechanical Engineer at Applied Materials Inc. in Bangalore, India. He received his Bachelors in Technology degree in Mechanical Engineering from the National Institute of Technology, Bhopal, India.



**Ghatu Subhash** is the Newton C. Ebaugh Professor in the Department of Mechanical and Aerospace Engineering at the University of Florida. His research expertise is in the broad area of solid mechanics with emphasis on multiaxial constitutive response of advanced materials, high strain rate behavior, experimental solid mechanics and process-structure relationships. He is a fellow of ASME and SEM. He currently serves as the associate editor of *J Am Cer Soc, Mech Mater*, and *J Eng Mater Tech*. He has recently received M.M Frocht Award from *Exp Mech*, ORR Best Paper Award from *J Eng Mater Tech* and 'Significant Contribution Award' from the American Nuclear Society.



**Douglas Spearot** is an Associate Professor in the Department of Mechanical & Aerospace Engineering at the University of Florida. His research focuses on the use of atomistic and mesoscale simulation techniques to study the mechanical and thermodynamic properties of materials. Dr. Spearot was awarded the NSF CAREER Award to elucidate the nanoscale mechanisms associated with phase nucleation during physical vapor deposition. Dr. Spearot received his Bachelors of Science in Mechanical Engineering from the University of Michigan. He completed his Masters of Science and Ph.D. degrees in Mechanical Engineering from the Georgia Institute of Technology.